



Norwegian University of  
Science and Technology

# Subsea Chemical Storage and Injection Station - Single line batch re-supply of chemicals

An experimental investigation into  
displacement mechanisms and separation  
methods

**Kjell Håvard Fjeldsaunet**

Subsea Technology

Submission date: June 2018

Supervisor: Tor Berge Gjersvik, IGP

Co-supervisor: Sigbjørn Sangesland, IGP

Norwegian University of Science and Technology  
Department of Geoscience and Petroleum



---

# Summary

This thesis seeks to simplify the re-supply process of a subsea chemical storage and injection (SCS&I) station by identifying possible alternative transport solutions. Specifically, this thesis explores the technical solution of sending several liquids in succession through a single line without mixing occurring between the different liquids.

The thesis explores using a polymer gel as a spacer liquid between the chemicals. To decide which polymers might be a good fit, several experts were contacted. The possible spacer fluid selected for testing was Xanthan gum (XG). This is a non-toxic polymer already in use in the oil and gas industry.

Three experiments were initially designed. Experiment 1 explores how the spacer liquid's viscosity evolves over time. When used in the transport system, the spacer fluid might spend some time in the pipe. If its properties were to change, this would have to be accounted for. Apart from one sample, the XG gel seemed stable both at room temperature storage and cold storage. However, mold developed on the samples with the lowest XG concentration after a month. The reason could be exposure to air or contamination during testing. So, another experiment, experiment 3, was designed to counter this effect.

Experiment 2 investigates how the XG gel reacts with the production chemicals that will be transported with this system in a static environment. This is to ensure compatibility of the chemicals during transport. Testing against glycol showed some initial dissolving of the XG gel, but the mix stabilized after a few days and seemed to not mix any further. Testing against other chemicals was not achieved during the work on this thesis.

Experiment 3 is a continuation of experiment 1, but it seeks to eliminate the effect of exposing the sample to air. When in use in the system, the XG gel will not be exposed to air, and if this exposure is the cause of the mold, this problem is not relevant for the final system. As a further improvement on experiment 1, temperature measurements are conducted simultaneously as viscosity measurements. In experiment 1 the temperature is only measured once before the viscosity measurements. The results of experiment 3 were much the same as experiment 1, the sample seemed stable over time, and a significant correlation was found between viscosity and temperature.

Experiment 4 investigates how the spacer liquid reacts with production chemicals in a dynamic setting, as well as the ability of the spacer liquid to keep the production chemicals separate during transport. A rig was designed and built in the hall laboratory. It consists of a tube shaped as a U with pressure applied on each end. The spacer liquid is put into the tube and placed in the middle of the tube, then the injection chemicals are placed on each side of the spacer liquid. Pressure is applied alternately at the ends of the tube, resulting in a back and forth fluid flow.

Experiment 4 showed that it was hard to keep the spacer liquid from mixing with the other chemicals in a dynamic environment. Higher concentration gels were tried to see if the higher viscosity would help, and a longer tube was tried in order to see if a less frequent change of direction would result in less mixing.

Keeping the chemicals separate using a Xanthan gum gel was not successfully achieved

---

in this thesis. However, the matter is not closed, and further work is needed before a final conclusion is reached. Future work should further investigate Xanthan gum gel as a spacer liquid. New experiments should be designed where the liquids are propelled by a pump rather than pressurized air to make the test conditions more realistic. Other candidates for spacer liquids should also be investigated, especially cross-linked polymers.



---

# Sammendrag

Denne masteroppgaven forsøker å forenkle påfyllingsprosessen til en kjemisk lagrings og injiserings-modul designet for å stå på havbunnen. Dette skal oppnås ved å identifisere en mulig alternativ transport-løsning. Mer spesifikt skal denne oppgaven prøve å finne en teknisk løsning for å sende ulike kjemikalier etter hverandre gjennom ett rør uten at kjemikaliene blandes.

Oppgaven undersøker om en polymer gel kan brukes for å separere kjemikaliene under transport. Eksperter ble kontaktet for å finne mulige kandidater for en separasjonsvæske. Valget falt til slutt på Xanthan gum. Dette er en ikke-giftig polymer som allerede er i bruk i olje- og gassindustrien.

Tre eksperimenter ble planlagt. Eksperiment 1 undersøker hvordan Xanthan gum gelens viskositet utvikler seg over tid, siden gelen kan bli liggende i transportrøret en stund. I røret på havbunnen vil gelen bli utsatt for lave temperaturer, og derfor skal eksperiment 1 se hvordan Xanthan gum gelens viskositet også holder seg ved temperaturer lik de den vil utsettes for på havbunnen. Med unntak av n prøver virket Xanthan gum gelen stabil over tid og ved kaldere temperaturer. Men prøvene med lavest Xanthan gum konsentrasjon utviklet etterhvert mugg, så eksperiment 1 ble avsluttet tidlig. Eksperiment 3 ble så planlagt som en oppfølger til eksperiment 1, og skulle unngå forholdene som førte til mugg.

Eksperiment 2 undersøker hvordan Xanthan gum gelen reagerer når den utsettes for kjemikaliene som skal transporteres. Dette skal sørge for at gelen er kompitabel med kjemikaliene som skal transporteres. Når den ble utsatt for glykol løste litt av gelen seg opp ganske raskt. Etter noen dager virket blandingene stabil for alle konsentrasjoner, og den resterende gelen løste seg ikke.

Eksperiment 3 er en fortsettelse av eksperiment 1. Dette eksperimentet søker å eliminere dannelsen av mugg, som observert i eksperiment 1. Her blir en større mengde gel blandet ut og delt i mindre prøver. Disse prøvene blir tatt ut av lagring og testet kun n gang. Her måles også temperaturen av prøven samtidig som viskositeten. Dette er for å få et klarere bilde av sammenhengen mellom temperatur og viskositet. Som i eksperiment 1 virket det som om viskositeten til prøven holdt seg stabil over tid.

Eksperiment 4 ser på hvordan separeringsvæsken reagerer ved eksponering mot produksjonskjemikaliene, og hvordan separeringsvæsken blander seg med produksjonskjemikaliene i et dynamisk miljø. Her ble det bygget en rig for simulering av transport. Denne består av en gjennomsiktig slange formet som en U. Kjemikaliene blir dyttet frem og tilbake av lufttrykk i slangen, og holdes separert av separasjonsvæsken. Lengden på fasen med separasjonsvæsken måles før og etter kjøring. Eksperiment 4 viste at en separeringsvæske av 0.5wt% Xanthan gum ikke klarte å holde kjemikaliene separert. Høyere konsentrasjoner ble forsøkt for å se om høyere viskositet kunne hjelpe. Lengre rør ble også forsøkt for å undersøke om færre forandringer i strømningsretning resulterte i mindre blanding av væskene. Men resultatene av disse forandringene viste ingen forbedringer.

I denne oppgaven ble ikke målet om å holde kjemikaliene separert ved bruk av en Xanthan gum gele nådd. Men flere undersøkelser bør gjøres før Xanthan gum gele avskrives

---

som kandidat til separeringsvæske. Eksperimenter hvor væskene drives av en pumpe fremfor lufttrykk, burde designes og gjennomføres. Videre kan man også undersøke andre kandidater til separeringsvæske, spesielt burde man fokusere på polymerer med krysskoblinger.

---

# Preface and Acknowledgements

This is a Master's thesis written by Kjell Håvard Fjeldsaunet at the Department of Geoscience and Petroleum at the Norwegian University of Science and Technology. The submission of this thesis concludes the two-year Master's degree program in Subsea Technology.

It has been two challenging years, and I have learned a lot and grown as a person. The thesis has allowed me to work with many subjects, and I feel I was able to use skills from all of my education.

I would like to thank my head supervisor Tor Berge Gjersvik and co-supervisor Sigbjørn Sangesland for their guidance and advice in the planning and execution of the work in this thesis. I would also like to thank the engineers without whom the work performed in the thesis would not have been possible: Noralf Vedvik, Roger Overå, and Steffen Wærnes Moen.

**Trondheim, 11.06.2018**

*Kjell Håvard Fjeldsaunet*

Kjell Håvard Fjeldsaunet

---

# Table of Contents

<b>Summary</b>	<b>i</b>
<b>Sammendrag</b>	<b>iii</b>
<b>Preface and Acknowledgements</b>	<b>v</b>
<b>Table of Contents</b>	<b>x</b>
<b>List of Tables</b>	<b>xi</b>
<b>List of Figures</b>	<b>xv</b>
<b>Abbreviations</b>	<b>xvi</b>
<b>1 Introduction</b>	<b>1</b>
1.1 Background . . . . .	1
1.2 Research Objectives . . . . .	2
1.3 Scope . . . . .	2
1.4 Structure of Thesis . . . . .	3
1.4.1 Chapter 1 - Introduction . . . . .	3
1.4.2 Chapter 2 - Theory . . . . .	3
1.4.3 Chapter 3 - Method . . . . .	3
1.4.4 Chapter 4 - Experimental Work . . . . .	3
1.4.5 Chapter 5 - Results . . . . .	3
1.4.6 Chapter 6 - Discussion . . . . .	3
1.4.7 Chapter 7 - Conclusions and Future Work . . . . .	3
<b>2 Theory</b>	<b>5</b>
2.1 Flow Assurance Challenges . . . . .	5
2.1.1 Hydrate . . . . .	5
2.1.2 Corrosion . . . . .	6
2.1.3 Scale . . . . .	6

---

2.1.4	Asphaltene . . . . .	7
2.1.5	Emulsions . . . . .	8
2.1.6	Wax . . . . .	8
2.1.7	Biocides . . . . .	9
2.2	Polymer Fundamentals . . . . .	10
2.2.1	PVC . . . . .	11
2.2.2	Xanthan Gum . . . . .	11
2.3	Fluid Mechanics Fundamentals . . . . .	11
2.3.1	Viscosity . . . . .	11
2.3.2	Couette flow . . . . .	13
2.3.3	Pressure Loss in Pipes . . . . .	13
2.4	Valves . . . . .	14
2.5	Pumps . . . . .	15
2.5.1	Gear Pump . . . . .	15
2.5.2	Progressive Cavity Pump . . . . .	16
2.5.3	Twin Lobe Pump . . . . .	16
2.5.4	Sliding Rotor Vane Pump . . . . .	16
2.5.5	Single Stage Centrifugal Pump . . . . .	17
2.5.6	Twin Screw Pump . . . . .	17
2.6	Statistics . . . . .	17
2.6.1	Basics . . . . .	18
2.6.2	Correlation Analysis . . . . .	18
<b>3</b>	<b>Method</b> . . . . .	<b>21</b>
3.1	Work-Structure . . . . .	21
3.2	Identifying Spacer Liquid . . . . .	22
3.3	Experiments . . . . .	22
3.3.1	Experiment 1 - Viscosity and Density Over Time . . . . .	22
3.3.2	Experiment 2 - Chemical Compatibility . . . . .	23
3.3.3	Experiment 3 - Viscosity and Density Over Time - Extended . . . . .	23
3.3.4	Experiment 4 - Spacer Liquid Performance . . . . .	24
3.4	Equipment Used in This Thesis . . . . .	25
3.4.1	Fann Viscometer Model 35SA . . . . .	25
3.4.2	Hamilton Beach Mixer . . . . .	27
3.4.3	Baroid Mud Balance . . . . .	27
3.4.4	Sartorius Quintix Model 224 . . . . .	28
3.4.5	LabVIEW . . . . .	28
<b>4</b>	<b>Experimental Work</b> . . . . .	<b>31</b>
4.1	Deciding on Separator Liquid . . . . .	31
4.2	Experiment 1 - Viscosity and Density Over Time . . . . .	32
4.2.1	Approach . . . . .	32
4.3	Experiment 2 - Chemical Compatibility . . . . .	33
4.3.1	Acquiring Chemicals . . . . .	33
4.3.2	Approach . . . . .	34
4.4	Experiment 3 - Viscosity and Density Over Time - Extended . . . . .	34

---

4.4.1	Viscosity Measurements . . . . .	35
4.4.2	Density . . . . .	36
4.5	Experiment 4 - Spacer Liquid Performance . . . . .	36
4.5.1	Modifications . . . . .	39
<b>5</b>	<b>Results</b>	<b>43</b>
5.1	Experiment 1 - Viscosity and Density Over Time . . . . .	43
5.1.1	Viscosity Measurements . . . . .	43
5.1.2	Density Measurements . . . . .	44
5.1.3	Mold Development . . . . .	45
5.2	Experiment 2 - Chemical Compatibility . . . . .	46
5.3	Experiment 3 - Viscosity and Density Over Time - Extended . . . . .	47
5.4	Experiment 4 - Spacer Fluid Performance . . . . .	48
5.4.1	Results From Modified Runs . . . . .	50
5.4.2	Residue in Tube . . . . .	51
<b>6</b>	<b>Discussion</b>	<b>53</b>
6.1	Experiment 1 - Viscosity Over Time . . . . .	53
6.2	Experiment 2 - Chemical Compatibility . . . . .	54
6.2.1	Exposure to Glycol . . . . .	54
6.3	Experiment 3 - Viscosity and Density Over Time - Extended . . . . .	55
6.3.1	Comparing results to experiment 1 . . . . .	56
6.4	Experiment 4 - Spacer Fluid Performance . . . . .	56
6.4.1	Rigging . . . . .	56
6.4.2	Running Experiment . . . . .	57
6.4.3	Effect of Residue in Tube . . . . .	61
<b>7</b>	<b>Conclusion and Future Work</b>	<b>63</b>
7.1	Conclusion . . . . .	63
7.2	Future Work . . . . .	64
7.2.1	Continue Testing of Xanthan Gum . . . . .	64
7.2.2	Evaluate Other Possible Spacer Liquids . . . . .	64
	<b>Bibliography</b>	<b>65</b>
	<b>Appendices</b>	<b>69</b>
<b>A</b>	<b>Tables</b>	<b>71</b>
<b>B</b>	<b>Results from Experiments</b>	<b>73</b>
B.1	Experiment 1 . . . . .	73
B.1.1	Viscosity Measurements . . . . .	73
B.1.2	Density Measurements . . . . .	77
B.2	Experiment 2 . . . . .	78
B.3	Experiment 3 . . . . .	80
B.4	Experiment 4 . . . . .	82
B.4.1	Initial Runs . . . . .	82

---

---

B.4.2 Higher Concentration Runs . . . . .	83
<b>C LabVIEW Programming</b>	<b>85</b>



# List of Tables

3.1	Fann Viscometer Speed Settings. . . . .	26
5.1	Results from initial runs of experiment 4. . . . .	49
6.1	Calculated viscosities at different temperatures . . . . .	55
6.2	Pressure drops for different XG gel concentrations over a 30km long pipe. . . . .	58
A.1	RPM and corresponding shear rate in $s^{-1}$ for the Fann viscometer. . . . .	71
A.2	Rotor - Bob Factors for the Fann viscometer. . . . .	71
A.3	Speed factors for the Fann viscometer. . . . .	72
B.1	Viscosity measurements 1.5wt% XG solution, room temperature storage . . . . .	73
B.2	Viscosity measurements 1.5wt% XG solution, cold storage . . . . .	74
B.3	Viscosity measurements 1wt% XG solution, room temperature storage . . . . .	74
B.4	Viscosity measurements 1wt% XG solution, cold storage . . . . .	75
B.5	Viscosity measurements 0.5wt% XG solution, room temperature storage . . . . .	75
B.6	Viscosity measurements 0.5wt% XG solution, cold storage . . . . .	76
B.7	Density measurements for experiment 1 . . . . .	78
B.8	Viscosity measurements 0.5wt% XG solution, cold storage . . . . .	80
B.9	Squared correlation coefficients for results from experiment 3. . . . .	80
B.10	Density measurements from experiment 3. . . . .	81

---

---

# List of Figures

1.1	Liquids in succession in a pipe. . . . .	2
2.1	A large gas hydrate plug formed in a subsea hydrocarbon pipeline (Heriot-Watt University, 2017) . . . . .	6
2.2	Scale crystals in pipe (Mackay, 2008) . . . . .	7
2.3	Asphaltene Solvent (SkySpring, Oil and Gas Service, Inc, 2017) . . . . .	8
2.4	Water-in-oil emulsion . . . . .	9
2.5	Wax deposition (The University of Kansas, 2017) . . . . .	9
2.6	Pitting corrosion due to MIC in a carbon steel water pipe (Skovhus et al., 2017) . . . . .	10
2.7	Left: Shear rate versus shear stress. Right: Shear rate versus viscosity. Source: Darby (2001) . . . . .	12
2.8	Velocity profiles of different viscosity models. Source: rheosense.com (2018) . . . . .	12
2.9	Couette flow. Source: Wikipedia (2018a) . . . . .	13
2.10	Left: External Gear Pump. Right: Internal Gear Pump. Source: Wikipedia (2018b) . . . . .	16
2.11	Lobe pump. Source: Wikipedia (2018c) . . . . .	16
2.12	Sliding rotor vane pump. Source: Wahren (1997). . . . .	17
2.13	Twin screw pump. Source: Wahren (1997) . . . . .	17
3.1	Flowchart of the work-structure for this thesis. . . . .	21
3.2	Form used for experiment 1. . . . .	23
3.3	Form used for experiment 3. . . . .	24
3.4	Form used in experiment 4. . . . .	25
3.5	Fann Viscometer. . . . .	26
3.6	Baroid Mud Balance. . . . .	27
3.7	Sartorius Quintix Model 224. . . . .	28
3.8	Left: Front panel of valve control. Right: Block diagram of valve control. . . . .	29
4.1	Setup for viscosity measurements . . . . .	35

---

4.2	Experiment 4 test set-up. . . . .	37
4.3	Model showing travel length $L$ for the test loop . . . . .	38
4.4	Loading device. . . . .	38
4.5	Loading Procedure . . . . .	39
4.6	The first 100-meter solution . . . . .	40
4.7	Second 100-meter solution . . . . .	41
5.1	Viscosity at different shear rates . . . . .	43
5.2	Viscosity over time at 300RPM, $511s^{-1}$ . . . . .	44
5.3	Viscosity over time at 3 RPM, $5.1s^{-1}$ . . . . .	44
5.4	Left: Bubbles right after mix. Right: Bubbles after two weeks. . . . .	45
5.5	Mold in sample . . . . .	46
5.6	Bottles with 100ml gel and 100ml glycol. From left to right: 1.5wt%, 1wt%, 0.5wt% . . . . .	47
5.7	Bottles with 100ml gel and 100ml glycol. From left to right: 1.5wt%, 1wt%, 0.5wt% . . . . .	47
5.8	Viscosity measurements from experiments 1 and 3 at $170s^{-1}$ . . . . .	48
5.9	Viscosity measurements from experiments 1 and 3 at $511s^{-1}$ . . . . .	48
5.10	Left: Gel-Glycol transition before run. Right:Gel-Glycol transition after run. . . . .	49
5.11	Gel migration . . . . .	50
5.12	Left: Border of residue can be seen. Right: Black writing behind residue compared to black writing behind no residue. . . . .	51
6.1	Air trapped in tube. . . . .	57
6.2	Pressure drop (bar) of different concentration XG gel at different transport lengths (m). . . . .	58
6.3	Loop Design for Improved Experiment . . . . .	60
A.1	Pearson Correlation Table (Carlson and Winqvist, 2017). . . . .	72
B.1	Correlation table for measurements on the 1.5wt% sample at room storage. . . . .	76
B.2	Correlation table for measurements on the 1.5wt% sample at cold storage. . . . .	76
B.3	Correlation table for measurements on the 1wt% sample at room storage. . . . .	77
B.4	Correlation table for measurements on the 1wt% sample at cold storage. . . . .	77
B.5	Correlation table for measurements on the 0.5wt% sample at room storage. . . . .	77
B.6	Correlation table for measurements on the 0.5wt% sample at cold storage. . . . .	77
B.7	All bottles on day of mix. . . . .	78
B.8	All bottles 7 days after mix. . . . .	79
B.9	All bottles 30 days after mix. . . . .	79
B.10	Comparison of results from experiment 1 and 3. . . . .	80
B.11	Correlation table for measurements in experiment3. . . . .	81
B.12	Results from initial runs of experiment 4. . . . .	82
B.13	Results from runs of experiment 4 with higher concentration XG gels. . . . .	83
B.14	Pressure drop calculations for different viscosities . . . . .	84

---

---

C.1	Block diagram for the valve control automation. . . . .	85
C.2	Left: Collapsed <i>Elapsed Time</i> sub-VI. Right: Expanded <i>Elapsed Time</i> sub-VI. . . . .	86
C.3	Valve control block diagram with numbered elements. . . . .	87
C.4	Valve control front panel with numbered elements. . . . .	87
C.5	Valve control block diagram with numbered elements. . . . .	89

---

# Abbreviations

XG	=	Xanthan Gum
SCS&I	=	Subsea Chemical Storage and Injection
RPM	=	Revolutions Per Minute
wt%	=	Weight Percentage
PVC	=	Poly(Vinyl-Chloride)

# Introduction

This chapter presents the background for this thesis, as well as research objectives, scope, and structure of the thesis.

## 1.1 Background

Today, the industry standard for subsea well control is hydraulic technology. The world's first all-electric subsea well started production on 4 August 2016, consisting of an electrically controlled Christmas tree, electrically controlled downhole safety valve, and electric subsea control modules. The main driver for this development was cost reduction. Removing the hydraulic pressure lines from an umbilical can reduce costs by over 15% for a 30 km step-out (Schwerdtfeger et al., 2017).

In 2014, Beaudonnet and Peyrony (2014) presented two case studies (one for an oil development and one for a gas development) where they investigated the removal of all hydraulic lines in the umbilical. They found that costs could be reduced by 80% for the oil case, and by 60% for the gas case. To achieve this, they proposed that injection chemicals were delivered by a subsea chemical storage and injection (SCS&I) station, and hydraulic pressure controls were replaced by electric controls. They proposed a solution for the SCS&I station where empty tanks were replaced with full tanks every six months.

Lundal and Festøy (2017) studied the SCS&I solution, as proposed by Beaudonnet and Peyrony (2014), in their Master's thesis. They found that the volume of such a solution would be in the order of  $5000m^3$ . This leaves a large footprint as well as represent a significant investment.

A possible solution that would reduce the amount of storage needed, and thereby the size of the module, is to transport the chemicals to the SCS&I in a cable. This solution will drastically reduce the rate of intervention needed as well. However, using current technology for delivery will negate the benefit of a simpler umbilical design. This thesis will therefore focus on a technical solution which will allow production chemicals to be transported in succession through a single line, and thereby significantly simplify the umbilical design.

## 1.2 Research Objectives

The problem description for this thesis is: Consider different methods for keeping injection chemicals separated during transport to a subsea chemical storage and injection station (SCS&I). Construct an experimental setup to conduct experiments to investigate the efficiency of the methods, and determine which is most suited for the further development of the SCS&I.

It is assumed that there needs to be some element that physically keeps the liquids separate. Using a mechanical solution presents a problem of storage and retrieval of the mechanical spacers after use. This thesis will therefore focus on a solution where a liquid is used as a spacer. Figure 1.1 shows a simple model of how the liquids will be transported in succession through a single line.

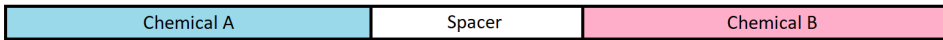


**Figure 1.1:** Liquids in succession in a pipe.

For this thesis the problem description is separated into the following objectives:

1. Identify possible spacer liquids
2. Investigate if possible spacer liquid:
  - (a) Can keep liquids separated during transport
  - (b) Is compatible with production chemicals

## 1.3 Scope

This thesis will only concern itself with the technical solution to the problem of transporting several liquids in a single line without the liquids mixing. The overall system solution, i.e. how the pipes are placed into the line in succession, how they are dealt with upon arrival to their destination, and how this system will connect with existing infrastructure, is not part of this thesis. However, some places it might be necessary to take the system solution into consideration with regards to parameters used in the experiments and to confirm the suitability of a spacer fluid. The information used for this will be gathered from the Master's thesis of Magnus Lund-Tønnesen.

For a broader view of the system solution, this thesis should be seen in conjunction with the Master's thesis of Magnus Lund-Tønnesen. The overall combined objective of these projects is to reduce the size of the SCS&I solutions suggested by Lundal and Festøy (2017), and Beaudonnet and Peyrony (2014).



## **1.4 Structure of Thesis**

This section gives a brief outline of the structure of this thesis and provides a brief summary of each chapter.

### **1.4.1 Chapter 1 - Introduction**

Chapter 1 provides the background for this thesis and presents the thesis' objectives.

### **1.4.2 Chapter 2 - Theory**

Chapter 2 gives the necessary theoretical information for further reading of the thesis. It starts with an overview of some flow assurance challenges faced by the oil and gas industry, and how these are combated. It continues with some information on polymers and explains some fluid mechanic concepts that affect the work in this thesis. Finally, it explains some statistical concepts used to evaluate the results of the experimental work.

### **1.4.3 Chapter 3 - Method**

Chapter 3 explains the structure of the work in this thesis. It also explains the reasoning behind the experiments and presents the design of the experiments.

### **1.4.4 Chapter 4 - Experimental Work**

Chapter 4 details the experimental work as it is carried out for this thesis. It outlines the execution of the experiments and provides reasons for changes and modifications that were done to the experiments.

### **1.4.5 Chapter 5 - Results**

Chapter 5 presents the results of the experiments outlined in chapter 4.

### **1.4.6 Chapter 6 - Discussion**

Chapter 6 discusses the results from chapter 5 and puts them into context with the overall objectives as presented in section 1.2.

### **1.4.7 Chapter 7 - Conclusions and Future Work**

Chapter 7 presents the conclusions reached through the discussion in chapter 6, and gives recommendations for future work.



# Theory

This chapter will explain some theoretical concepts that are necessary to understand the work presented in this thesis.

## 2.1 Flow Assurance Challenges

In the fall semester of 2017, a pre-study for this thesis was written as a specialization project together with Magnus Lund-Tønnesen (Fjeldsaunet and Lund-Tønnesen, 2017). This section is taken from this project.

The oil and gas industry is facing several challenges regarding formation of blockage and unstable flow along the production pipeline. This section will present a selection of the most common challenges, and how to combat them.

### 2.1.1 Hydrate

Gas hydrates are ice-like clathrate solids formed from water and small hydrocarbons (methane, ethane, propane, nitrogen, carbon dioxide and hydrogen sulfide) at relatively high pressures and low temperatures. They occur most commonly during drilling and production processes, and they can form anywhere to any time when water, natural gas, low temperatures, and high pressures are present (Kelland, 2014a). Figure 2.1 shows a hydrate plug that has formed in a subsea pipeline. Hydrates can be prevented by chemical treatment which includes the use of chemical inhibitors, where methanol (MeOH) and monoethylene glycol (MEG) are the most common.

Hydrate formation can also be prevented if enough water can be removed from the production fluids. Thermal insulation aims to maintain the temperature above hydrate formation conditions. Depressurization is applied on both sides of the hydrate plug to avoid it breaking loose and becoming a dangerous projectile, but this is not a good solution for deepwater installation due to high hydrostatic pressures of the water (Kelland, 2014a). There are several methods that can increase the temperature in the pipe. For example, active heating can be applied either with electricity or using a double pipe and circulating

hot fluid on the outside of the production line. One can also bury the pipe or put insulating material around it. However, heating is an expensive alternative and is mostly used only in special circumstances (Kelland, 2014a).



**Figure 2.1:** A large gas hydrate plug formed in a subsea hydrocarbon pipeline (Heriot-Watt University, 2017)

## 2.1.2 Corrosion

Bai and Bai (2010a) define corrosion as *the deterioration of a metal due to chemical or electrochemical interactions between the metal and its environment* (Bai and Bai, 2010a). It can happen both internally and externally, where internal corrosion is caused by the presence of CO<sub>2</sub>, H<sub>2</sub>S, water, and organic acids in production fluids. The level of corrosion depends on the environment and metal in use. External corrosion of a metal occurs due to general exposure to water or atmosphere (Bai and Bai, 2010a).

Internal corrosion can be prevented by using internal coatings. These also reduce the friction which improves the flow efficiency. Another way to prevent internal corrosion is by injecting corrosion inhibitors. These are chemicals that reduce the corrosion rate by adsorbing themselves to the metal surface as a film. External corrosion can be reduced by either applying an organic coating or by using cathodic protection. Cathodic protection can work in two ways. It can work either by applying a sacrificial anode to the metal to be protected or by applying an impressed current connection between the anode and the cathode (metal to be protected). The most effective solution is a combination of these two, however, this is not always the most cost-effective solution. (Bai and Bai, 2010a)

## 2.1.3 Scale

Scale is formed when ions in the produced water form salts due to pressure or temperature changes. These salt-crystals may precipitate on the pipe walls. The most common type of scale is formed from calcium carbonate (Bai and Bai, 2010b; Kelland, 2014b). Scale will form along the whole of the circumference of the pipe wall. If it grows sufficiently, it will effectively reduce the diameter of the pipe, and constrict the flow, as can be seen in figure 2.2. This can be identified by an increased pressure drop along the pipe.



**Figure 2.2:** Scale crystals in pipe (Mackay, 2008)

Scale is dealt with either proactively with chemical inhibition, or reactively with regular mechanical cleaning. The most common way to deal with scale is the use of scale inhibitors (Bai and Bai, 2010b). Chemical inhibition is done either by injecting scale inhibitors into the production flow, injecting scale inhibitors into the reservoir where the inhibitors adsorb into the reservoir rock, or by depositing solid scale inhibitors in the reservoir. The latter two are called squeeze treatment, and the inhibitor is released as the reservoir is produced (Kelland, 2014b).

Chemical treatment works by either stopping the nucleation process where the scale crystals are formed or by hindering the formed crystal from growing. The latter may be achieved by the chemicals reacting with the crystal structure, or by hindering the crystals in depositing on the pipe walls. Bai and Bai (2010b) list the most common scale inhibitors as inorganic polyphosphates, organic phosphates esters, organic phosphonates, and organic polymers.

#### 2.1.4 Asphaltene

Asphaltenes are black coal-like substances found in crude oil. They tend to be sticky which makes it difficult to remove them from surfaces. Asphaltenes can be found in all oils and their stability is influenced by the pressure, temperature and certain types of completion fluids.

Asphaltene problems occur infrequently offshore but can have a severe impact on project economics. Asphaltene deposition will most likely occur in the tubing when the temperature and pressure of the produced fluids pass the bubble point. To mitigate asphaltene problems the subsea system design generally relies on bottom hole injection of inhibitors. Asphaltene deposits are very difficult to remove once they occur. Bai and Bai (2010c) writes "Unlike wax deposits and gas hydrates, asphaltene formation is not reversible", however, Kelland (2014c) states that this is a controversial point, and some studies have shown that asphaltene flocculation might be reversible. Asphaltene deposition can be prevented when the asphaltene inhibitors (AI) are dosed at a very low concentration. In the absence of inhibitors, it is not uncommon with monthly cleanouts of the tubings (Bai and Bai, 2010c).



**Figure 2.3:** Asphaltene Solvent (SkySpring, Oil and Gas Service, Inc, 2017)

### 2.1.5 Emulsions

An emulsion is a mixture of two liquids where one is present as droplets suspended in another continuous liquid. Crude oil is normally produced as a water-in-oil emulsion (Kelland, 2014d). Here, water droplets are suspended in the continuous oil phase. To meet standards for selling and reduce corrosion of the pipeline, water must be removed from the oil. Traditionally, demulsifiers are added at the processing facilities, but the stability of an emulsion increases over time, and it may be more difficult to separate the liquids when they reach the separator, even when adding demulsifiers. Therefore, adding demulsifiers at the wellhead, or even downhole, may greatly improve the separation at the processing facilities (Kelland, 2014d).

Kokal (2002) mentions five different factors that affect emulsion stability: Emulsifiers present in crude oil, temperature, solids, droplet size, and pH.

Emulsifiers may exist naturally in crude oil, such as asphaltene or resins, or the emulsifying effect may come from injected chemicals. Emulsifiers are usually molecules consisting of a polar hydrophilic part and a non-polar hydrophobic part. This molecule will orient itself on the interface between the two phases, and form a film between the phases. Film forming corrosion inhibitors are often surfactants and may stabilize the emulsion. Therefore, careful selection of corrosion inhibitor may help reduce the amount of demulsifier needed (Kelland, 2014d).

Demulsification is achieved through a two-step process; flocculation and coalescence (Kokal, 2002). Flocculation is a process where droplets cling together without merging. Coalescence is the process where two or more drops merge into a bigger drop. These bigger drops are less stable and settle faster.

### 2.1.6 Wax

Wax is typically long-chains of alkane compounds naturally presented in crude oil. Deposition of wax on pipeline walls increases as the fluid temperature decreases. When the temperature gets below the cloud point, crystals will begin to form and accumulate on the pipe walls. Over time this results in flow restriction, or possibly a blockage of the pipeline, and thereby reducing the pipeline efficiency. (Bai and Bai, 2010c) The wax deposition thickness depends on temperature, pressure, composition of oil and velocity of the fluid (The University of Kansas, 2017).

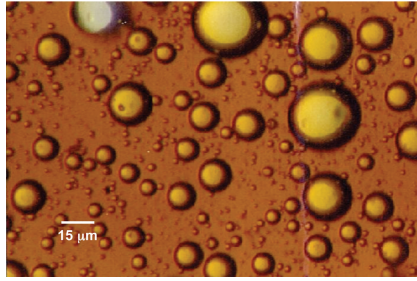


**Figure 2.4:** Water-in-oil emulsion

Wax control and management is conducted either by flowline pigging, thermal heating, inhibitor injection or by coiled tubing intervention. If the wax has formed, flowline pigging is mostly used. Chemical inhibitors can also be used, but these are often not effective and they tend to be expensive. In cases where pigging is not practical, the wax deposition is controlled by keeping the temperature over the cloud point for the whole flowline. (Bai and Bai, 2010c)



**Figure 2.5:** Wax deposition (The University of Kansas, 2017)

### 2.1.7 Biocides

When practicing corrosion control there are several corrosion mechanisms to consider. One of the mechanisms is microbiologically induced corrosion (MIC), which is estimated to account for 40% of internal corrosion in the oil and gas industry (Turkiewicz et al., 2013). The most common form of MIC is sulfate-reducing bacteria (SRB) (Wen et al., 2006). These are bacteria whose metabolic byproduct is hydrogen sulfide ( $H_2S$ ), which is highly corrosive, and may also bond to iron ions to make iron sulfide, a form of scale (Dickinson et al., 2005). Kelland (2014e) presents five main mechanisms to minimize reservoir souring by controlling SRB; Add biocide to kill SRB, treat SRB with a biostat, stimulate the formation of nitrate reducing sulfide-oxidizing bacteria (NR-SOB), use unsulfated aquifer or desulfated water in injection wells, and use an  $H_2S$  scavenger. Two of these mechanisms require chemical injection; biocides and biostats. Biocides are chemicals that kill the bacteria, and biostats are chemicals that hinder growth of the bacteria.

Kelland further states that the most effective application of biocides is a mix of one or more biocides, or of biocides and biostats.

There are mainly two classes of biocides (Kelland, 2014e); oxidizing and non-oxidizing. Oxidizing biocides work by causing oxidation/hydrolysis of protein groups in the bacteria. Non-oxidizing biocides work by disrupting the cell walls of the bacteria. Some SRB may be immune to some non-oxidizing biocides, while oxidizing biocides generally work on all SRBs. However, some oxidizing biocides may be corrosive, whereas non-oxidizing biocides are not corrosive, some may even be corrosion inhibiting. The selection of biocide treatment should, therefore, be planned for each field to find the optimum solution.



**Figure 2.6:** Pitting corrosion due to MIC in a carbon steel water pipe (Skovhus et al., 2017)

## 2.2 Polymer Fundamentals

Polymers are natural or synthetic substances consisting of large molecules which are multiples of smaller molecules. The smaller molecules are called monomers, and the large polymer molecules are called macromolecules. Macromolecules are also referred to as chains due to their structure. Naturally occurring substances such as proteins, cellulose and nucleic acids are polymers, as well as man made materials such as concrete, plastics and rubbers. A polymer which consists of a large number of monomers is sometimes called a high polymer. A polymer can be made of one kind of monomer and is then called a homopolymer. If the polymer consists of more than one kind of monomer it is called a copolymer (Encyclopædia Britannica, 2018). A cross-link is a link between four or more chains, either by a common monomer or a link consisting of an atom or a molecule (Jenkins et al., 1996).

Typical polymers are plastics, as all plastics are polymers. However, not all polymers are plastics. Over the last 50 years, the plastic industry has been one of the fastest growing industries, and polymer research has been extensive (Bourne, 2013). Polymers are also added to coatings to increase strength and adhesiveness (Buss et al., 2011). Polymers are, however, prone to degradation due to UV-light. Here the polymer chains are broken, and



in a coating the broken polymer may deposit on the coating as a white powder. This is known as chalking (Santos et al., 2005).

### 2.2.1 PVC

Poly(vinyl-chloride), or PVC, is a thermoplastic made by polymerization of the monomer vinyl-chloride. PVC is used for a range of applications, and additives are used to get the desired qualities. PVC offers excellent chemical resistance and is used in many industrial processes (Patrick, 2005)

### 2.2.2 Xanthan Gum

Xanthan gum (XG) is a high molecular weight polysaccharide produced by *Xanthomonas* bacteria. It was the second bacterial polysaccharide commercialized, and is as such one of the most extensively tested bacterial polysaccharides. It is non-toxic and allowed in food production. XG dissolved in water forms a pseudoplastic liquid (Sworn, 2009), meaning that viscosity decreases as shear rate increases. The viscosity is generally not affected by pH. XG is also relatively stable at different electrolyte concentrations in the solvent. Below 0.15 wt% XG, electrolytes decrease the viscosity somewhat, and above this concentration the addition of electrolytes has the opposite effect. Peak viscosity is here achieved at 0.02-0.07% concentration of sodium chloride. Increasing the electrolyte concentration above this does not effect the viscosity further (Kang and Pettitt, 1973).

In the oil and gas industry, XG is used as a viscosifier for drilling fluid. Its non-newtonian rheology creates a flat velocity profile in annular flow. This allows for a more efficient lift of cuttings (Schlumberger Oilfield Glossary, 2017). Cross-linking of XG have been shown to increase the viscoelasticity of a water soluble XG gel (Zhang et al., 2016).

In this thesis, XG is used to mean the polymer in near pure condition, usually in the form of powder. XG gel is used to mean a gel of XG dissolved in water. To differentiate gels of different XG concentration, the wt% of XG in the gel is used. For example, 1.5wt% XG gel means a gel consisting of 1.5% XG and 98.5% water by mass.

## 2.3 Fluid Mechanics Fundamentals

This thesis tries to identify a possible liquid spacer for a chemical transport system related to a proposed SCS&I. This section will explain some concepts and properties which is examined or mentioned in this thesis. Most information in this section is provided by Darby (2001). Where this is not the case, additional sources will be provided.

### 2.3.1 Viscosity

A large part of this thesis is concerned with the viscosity of the spacer fluid, and how this changes over time. Viscosity is "the property of resistance to flow in any material with fluid properties" (Merriam-Webster Online Dictionary, 2018). Most normal, simple liquids are newtonian fluids where viscosity is proportional to the relative rate of movement. This behaviour is described in equation 2.1.

$$\tau = \dot{\gamma}\mu \quad (2.1)$$

Here  $\tau$  is the shear stress,  $\dot{\gamma}$  is the shear rate, and  $\mu$  is the dynamic viscosity. If the relation is given as a more complex equation, the fluid is a non-newtonian fluid. There are several models describing the viscosity of non-newtonian fluids, and the relation between shear rate and shear stress, and shear rate and viscosity, for the different viscosity models is shown in figure 2.7.

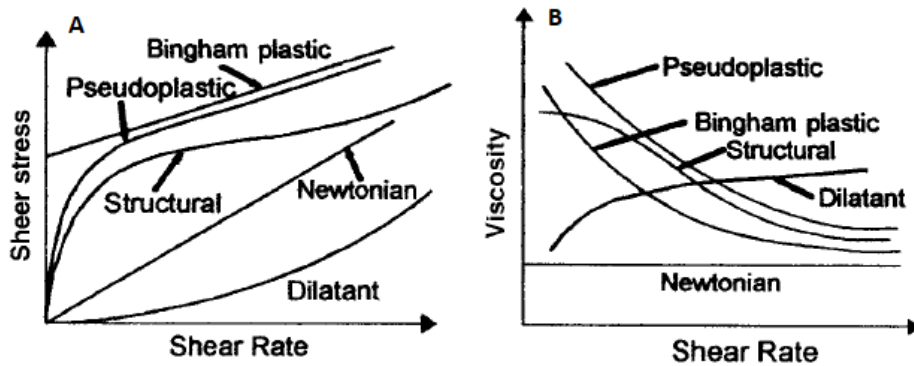


**Figure 2.7:** Left: Shear rate versus shear stress. Right: Shear rate versus viscosity. Source: Darby (2001)

The viscosity development has an impact on the flow of the fluid, especially the velocity profile during laminar flow. Figure 2.8 show how the velocity profiles of the different models. Shear thinning is equivalent to pseudoplastic, and shear thickening is also known as dilatant.

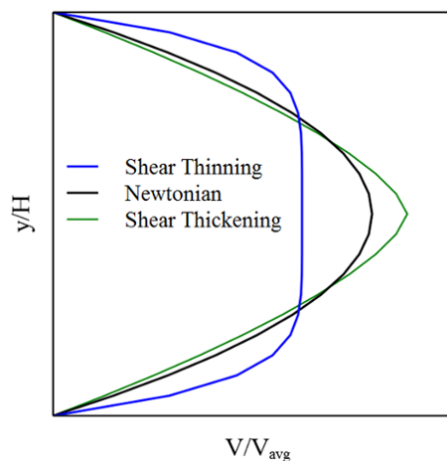


**Figure 2.8:** Velocity profiles of different viscosity models. Source: rheosense.com (2018)

Equation 2.2 can be used to calculate the nominal shear rate from flow velocity in a pipe (Holland and Bragg, 1995).

$$\dot{\gamma} = \frac{8v}{d} \quad (2.2)$$

Here  $v$  is the velocity and  $d$  is the diameter of the pipe. The velocity is given in  $m/s$  and the diameter in meters, meaning shear rate has the unit  $s^{-1}$ , or reciprocal seconds. For a non-newtonian fluid where viscosity will vary with changing shear rate, it is necessary to calculate the shear rate in order to find the viscosity at certain conditions. For instance, when calculating pressure drop in a pipe where a non-newtonian fluid is flowing.

### 2.3.2 Couette flow

Couette flow is the flow resulting from the motion of a flat plate parallel to another stationary flat plate where the gap between the plates is filled with liquid, as shown in figure 2.9. This effect can be used to evaluate properties of the fluid, such as viscosity.

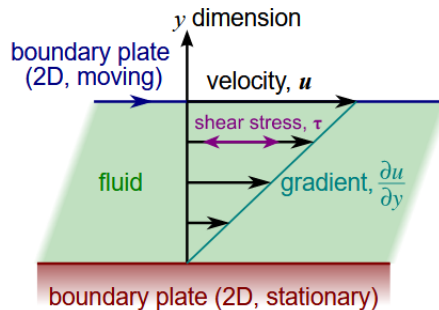


Figure 2.9: Couette flow. Source: Wikipedia (2018a)

### 2.3.3 Pressure Loss in Pipes

In the fall semester of 2017 a pre-study for this thesis was performed as a specialization project (Fjeldsaunet and Lund-Tønnesen, 2017). This section on the pressure loss in pipes is largely taken from this project. But the sources in the pre-study was lacking, so new sources are used and added for this thesis and are different from the original specialization project. The text has also been changed some places to better correspond to the new sources.

The pressure loss in a cylindrical pipe due to friction may be calculated using the Darcy-Weisbach equation (Ellenberger, 2014):

$$\frac{\Delta p}{L} = f_d \left( \frac{\rho}{2} \right) \left( \frac{v^2}{D} \right) \quad (2.3)$$

Here,  $f_d$  is the Darcy friction factor,  $v$  is the average fluid velocity which is usually used as volumetric flow rate divided by the wetted area of the pipe, and  $D$  is the diameter. This gives us the pressure loss per unit length ( $L$ ).

The Darcy friction factor is calculated using Reynolds number. Reynolds number is a dimensionless number introduced by George Stokes to classify the flow properties and is given as (Ellenberger, 2014):

$$Re = \frac{\rho U h}{\mu} \quad (2.4)$$

Here,  $\rho$  is density,  $U$  is velocity,  $\mu$  is viscosity, and  $h$  is the relevant linear dimension. For a pipe, the relevant linear dimension is the diameter, and it is customary to use  $d$ . For a flow with a Reynolds number below 2000, the flow is considered to be laminar. A Reynolds number between 2000 and 4000 is considered unsteady, and at values above 4000 the flow is considered turbulent. For laminar flow, the Darcy friction factor may be approximated as (Ellenberger, 2014):

$$f_d = \frac{64}{Re} \quad (2.5)$$

## 2.4 Valves

”A valve is a device that regulates the flow of a fluid by opening, closing, or partially obstructing the passageway in which it is installed” (Rennels and Hudson, 2012). An experiment in this thesis uses valves, so this section will explain the basics of valves.

Nesbitt (2007) divide valves into five main categories:

- Isolating Valves
- Non-Return Valves
- Regulators
- Control Valves
- Safety Relief Valves

Isolating valves are used to stop flow completely. This can be to stop flow when a pipe is damaged, or to remove flow from a section of a system to allow for maintenance or modification. Some common isolating valves are gate valve, ball valve, globe valve, and piston valve. Non-return valves are used to prevent back-flow. This is normally used to protect pumps and compressors that will break if they experience back-flow. Regulators and control valves are used to regulate pressure or flow-rate. The difference between regulators and control valves are that control valves are powered by an external source such as hydraulic, pneumatic or electric power, and regulators are manually operated. Safety relief valves will vent the system if the pressure surpasses a set threshold. A valve that is controlled electrically using the electromagnetic effects of a current through a coil, is called a solenoid valve (Nesbitt, 2007).

In this thesis, a pneumatic solenoid directional control valve is used. Here, a piston is moved by the induced magnetic field of the solenoid, and the position of the piston controls

the direction of the flow. A ball valve is also used in one part of the thesis. In this valve a ball sits in a housing, and there are holes bored in the ball. The position of the ball decides the flow. This valve can be used for regulation of flow-rates, or as a directional valve. A three-way ball valve is used in this thesis. They are classified according to the bore in the ball. An L-bore has an angled flow path through the ball. A T-bore has a T-shaped bore, and flow can come into the valve from two or one directions, and exit through one or two directions respectively. Lastly, a pneumatic membrane choke valve is used. This is a valve where the air flows past a membrane. Tightening the valve pushes the membrane down and chokes the flow. This results in lower pressure downstream from the valve.

## 2.5 Pumps

The use of pumps is discussed in this thesis. This section provides some background information that is relevant to this discussion.

Pumps convert mechanical energy to hydraulic energy. Pumps are usually classified into two main categories: Positive displacement pumps and dynamic pumps. Dynamic pumps deliver a continuous flow, but the flow-rate will vary according to the system-pressure. Positive displacement will deliver a constant flow-rate, but the flow will usually be pulsating. (Hydrauliske Pumper, 2000). Flanigan et al. (1988) examined the shear of five different types of pumps:

- Progressive cavity pump
- Twin lobe pump
- Sliding rotary vane pump
- Single stage centrifugal pump
- Twin screw pump

This section will look at each of these pumps more closely. Gear pumps will also be presented in this section as they are also discussed. In the list above, the pumps are listed by amount of shear from least to most Flanigan et al. (1988).

### 2.5.1 Gear Pump

Gear pumps use the meshing of gears to propel the liquid. One gear is driving the rotation of both gears (Hydrauliske Pumper, 2000). Figure 2.10 shows the two main types of gear pumps, external and internal. The red arrows show the flow path in each of the pumps.

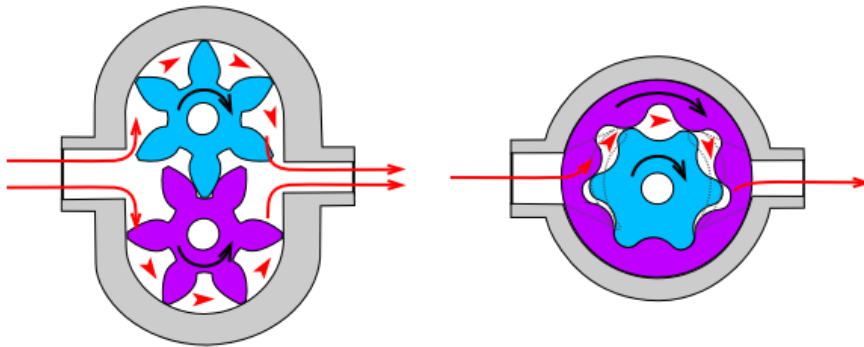


**Figure 2.10:** Left: External Gear Pump. Right: Internal Gear Pump. Source: Wikipedia (2018b)

### 2.5.2 Progressive Cavity Pump

A progressive cavity pump pushes liquids by rotating a single helix rotor inside a double helix profile. This forms cavities between the outer shell and inner rotor which moves forward (Wahren, 1997). Flanigan et al. (1988) found that this pump was the pump which exerted the lowest shear on the pumped fluid.

### 2.5.3 Twin Lobe Pump

Lobe pumps work much like a gear pump. However, in a lobe pump one lobe does not drive the other. The lobes are independently driven, and timing allows the operation. Figure 2.11 shows a model of a three-lobed pump. A twin lobe pump has two lobes on each rotor.

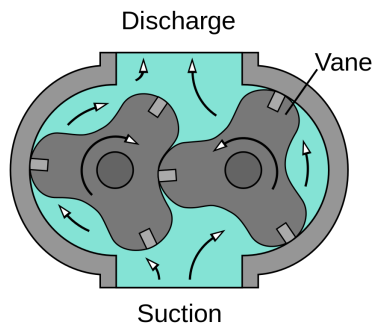


**Figure 2.11:** Lobe pump. Source: Wikipedia (2018c)

### 2.5.4 Sliding Rotor Vane Pump

[H] Sliding rotor vane pumps consist of a rotor inside a circular casing. The rotor contains vanes which slide out due to centrifugal forces, and are pushed in by the housing. The

vanes and housing form compartments which decrease in size as the rotor rotates, and are pushed out when the compartment is at its smallest. This shown in figure 2.12.

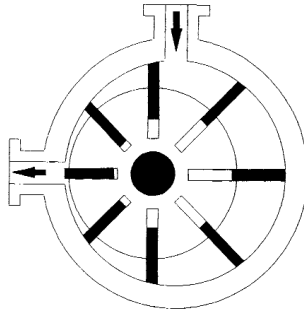


**Figure 2.12:** Sliding rotor vane pump. Source: Wahren (1997).

### 2.5.5 Single Stage Centrifugal Pump

A single stage centrifugal pump is a dynamic pump. It uses a single impeller for the propulsion of the fluids rather than several in series, which is called multi stage centrifugal pumps.

### 2.5.6 Twin Screw Pump

A twin screw pump uses two rotating screws. One is active and drives the other. Cavities are formed which move forward. Figure 2.13 shows a sketch of a twin screw pump.

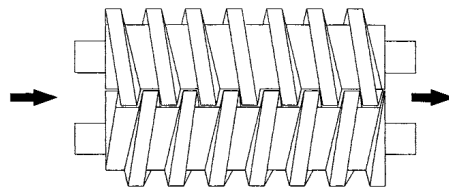


**Figure 2.13:** Twin screw pump. Source: Wahren (1997)

## 2.6 Statistics

Part of this thesis relies on measurements, and statistics can help determine the validity of the measurements. This section will describe the statistical methods used in this thesis.

## 2.6.1 Basics

This section provides definitions for basic statistical concepts. This is to avoid confusion in later chapters and establish how the concepts are used in this thesis. Most information in this section is gathered from Hand (2008). If other sources are used, this will be pointed out where necessary.

### Averages

An average is a representative value for a set of values. There are several types of averages. However, the most common one, and the one most people associate with the word average, is the *arithmetic mean*, or just *mean*. The arithmetic mean is calculated by dividing the sum of all values on the number of values, as shown in equation 2.6.

$$\bar{x} = \frac{1}{n} \sum_{i=1}^n x_i \quad (2.6)$$

Another form of average value is the *median*, and it is the middle value in a sorted set, or the arithmetic mean of the two middle values if  $n$  is an even number. The *mode* is another average value. This the number that occurs the most in the set.

In this thesis, we will mostly use the arithmetic mean. We will use the term *average*. If any other average value is used, this will be pointed out.

### Dispersion

The dispersion is a characteristic that tells us how the values in a set are distributed. A common value of dispersion is the *range*. This is simply the difference between the largest and smallest value. However, since this value is based solely on two values in the set, it might not describe the distribution sufficiently. The *variance* is the squared average difference between the average and each value. It is calculated as shown in equation 2.7.

$$\sigma^2 = \sum_{i=1}^n \frac{\bar{x} - x_i}{n} \quad (2.7)$$

The variance is squared so that negative and positive values will not cancel each other out. However, the unit of the variance is therefore the unit of the measured value squared. Therefore, it is common to use the *standard deviation* as a measure of dispersion. This is simply the square root of the variance. This can be viewed as a measure of how far from the mean a measurement can be expected to be.

## 2.6.2 Correlation Analysis

Correlation analysis is a tool used to investigate how variables relate to each other. This section outlines different methods and quantities used in correlation and regression analysis. The source for most of this section on correlation analysis will be Schroeder et al. (1986). If another source is used, this will be pointed out.



”The correlation coefficient measures the degree of linear association between two variables” (Schroeder et al., 1986). It ranges from 1 to  $-1$ , where higher absolute value represents a stronger association, and values closer to zero represent a weaker association. A negative coefficient of correlation equates to a negative correlation. Meaning, an increase in the independent value leads to a decrease in the dependent value.

There are several correlation coefficients, but the one normally used is the Pearson correlation coefficient. This is the correlation coefficient that will be used in this thesis. For this thesis Microsoft Excel is used to calculate correlation, and the Excel function CORREL gives the Pearson correlation coefficient. This is also the correlation coefficient that is calculated when the data analysis tool *Correlation* is used in Excel. The equation as given by Excel is shown in equation 2.8 (Microsoft, 2018).

$$\text{Correl}(x, y) = \frac{\Sigma(x - \bar{x})(y - \bar{y})}{\sqrt{\Sigma(x - \bar{x})^2(y - \bar{y})^2}} \quad (2.8)$$

To decide whether the correlation is statistically significant, a simple hypothesis test is performed. In a hypothesis test, two or more hypotheses are proposed. The null hypothesis,  $h_0$ , is the ”starting point”, the other hypotheses are called alternative hypotheses. Values are calculated for the rejection of the hypotheses. For a correlation analysis, the null hypothesis is that there is no relationship between the variables under investigation. Consequently, the alternative hypothesis is that there is a correlation.

The table shown in figure A.1 in the appendix shows the values for significant correlation coefficients. Here  $\alpha$  is the significance level and  $df$  is the degrees of freedom. The degrees of freedom is equal to  $N - 2$ . For example, if the sample size is 15, the degrees of freedom equals 13. Using the table in figure A.1 with the  $df$  equal to 13 and an  $\alpha$  of 0.05, a correlation coefficient of 0.441 or more indicates a significant relationship between the variables.

In chapter 5, t-tests are used to determine whether measurements from experiment 1 are different from the measurements from experiment 3. The t-test determines if the datasets have a significantly different average value. In Excel this is done using the T.TEST function. This function returns the p-value. The p-value is the probability that any difference observed is due to chance, and it is normal to use a confidence level of 95%. This means that a p-value of less than 0.05 suggests that there is a 95% chance or more that the differences are not due to chance, and we can reject the null hypothesis.

In chapter 6, the *Regression* data analysis tool is used to determine the correlation between viscosity, temperature and time. The regression analysis can take several variables. This tool is therefore useful in this case as it can calculate the adjusted correlation coefficient of several variables. The output of this tool includes R,  $R^2$ , and adjusted  $R^2$ . The R is the correlation coefficient,  $R^2$  is the squared correlation coefficient, and adjusted  $R^2$  is the squared correlation coefficient adjusted for multiple variables. Using this tool, we can calculate the adjusted  $R^2$ , and compare it to the correlation coefficients of each variable alone.



# Chapter 3

## Method

This chapter will describe the methods used in this thesis, and provide insight to the process used in this thesis. The equipment used in the experiments will also be introduced in this chapter.

### 3.1 Work-Structure

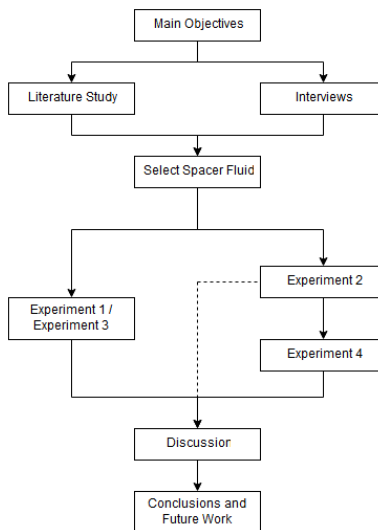


**Figure 3.1:** Flowchart of the work-structure for this thesis.

Figure 3.1 shows the structure of the work in this thesis. The main objectives are at the top as all work in this thesis stem from these. With these objectives in mind, a literature

study is performed to search for possible candidates for a spacer liquid. While this is done, interviews with experts are also performed. They are performed in person, over telephone, or via e-mail correspondence. On the basis of the literature study and the interviews, a decision is made on possible spacer liquids.

Experiment 1, and later experiment 3, is started right away when a possible spacer liquid is chosen. This is because these experiments will produce more robust results if they are conducted for as long as possible. Experiment 2 is started at the same time as experiment 1. This is a simple experiment, and if the spacer liquid fails this experiment, it is not a valid candidate for further research. If experiment 2 fails, experiment 1 or 3 is aborted, and experiment 4 is skipped for this specific spacer liquid candidate. The results from experiment 2 are discussed and conclusions are drawn.

If experiment 2 is successful, experiment 4 is conducted with the chosen spacer liquid. Experiment 1 and 3 will continue to run alongside experiment 4. Results are discussed, and then conclusions are drawn.

## **3.2 Identifying Spacer Liquid**

This part of the thesis utilizes qualitative methods. The data here is gathered through interviews, e-mail conversations, and literary review. These interactions provide information on which liquids may be candidates. The results of these inquiries are possible spacer liquids which will be studied further through the experiments outlined later in this chapter. This work concerns research objective 1.

## **3.3 Experiments**

### **3.3.1 Experiment 1 - Viscosity and Density Over Time**

The objective of this experiment is to investigate how a spacer liquid's properties evolve over time at different temperatures. The reason for this is that a spacer liquid might spend some time in the pipe, either by design or due to unexpected shut-downs. It is therefore necessary to investigate how the spacer liquid's properties change over time. If the properties change drastically, it might affect its ability to keep the liquids separate during transport. This experiment is therefore connected to research objective 2.a. The operation temperature of the system where the spacer liquid is used might vary. Therefore, the effect of temperature is also investigated.

The spacer liquid is prepared and divided into two samples. One is stored at room temperature. The other is stored in a refrigerator. Three times a week, the samples' viscosity is measured using a Fann viscometer. On the third measurement day, the density is measured as well.

The results are noted and analyzed to see whether there is a difference between the samples. To see whether the viscosity changes over time, a correlation analysis is performed. This analysis indicates whether there is a correlation between the age of the sample and the viscosity.

This experiment utilizes quantitative methods. Numerical data is collected and analyzed. Figure 3.2 shows the form used to register data.

The figure shows six identical data collection forms arranged in two rows of three. Each form is a table with the following structure:

Date:	Temp:
RPM	Measurement
$\Theta_3$	
$\Theta_{100}$	
$\Theta_{300}$	
$\Theta_6$	
$\Theta_{200}$	
$\Theta_{600}$	

**Figure 3.2:** Form used for experiment 1.

For this experiment to be as accurate as possible, steps should be taken to ensure that measurements are performed the same way each time.

### 3.3.2 Experiment 2 - Chemical Compatibility

The objective of experiment 2 is to investigate whether the spacer liquid is chemically compatible with the chemicals it will keep separate, research objective 2.b. To answer this, the spacer liquid is placed into a storage vessel together with samples of the chemicals it will be exposed to. The samples are observed over time, and photos are taken to document the evolution of the samples.

This experiment is a quantitative experiment, but the values measured are not numerical. It is still a quantitative experiment as it is possible to design an experiment where the results are quantified. However, this seemed excessive for our purposes, and a simpler design was chosen. The experiment relies on visual observation which means it is prone to bias and misinterpretation. Photos are taken of the samples in order to simplify discussion and allow others to examine and scrutinize the results.

### 3.3.3 Experiment 3 - Viscosity and Density Over Time - Extended

This experiment is an extension of experiment 1. Due to observations made in experiment 1, there was a need for an improved version of the experiment. The objectives of this experiment are the same as in experiment one.

There are a few differences from experiment 1. Firstly, a larger batch of spacer liquid is prepared. This batch is split into several samples. Measurements are only performed once on each small sample, and the sample is subsequently discarded. This is done to limit the spacer liquid's exposure to air. Secondly, the temperature is measured simultaneously

as the viscosity. This is to get a more accurate evaluation of the relation between viscosity and temperature.

One further alteration was made from experiment 1 to experiment 3. The samples are only stored in cold storage. Experiment 1 found that there is only a small variation of viscosity due to the difference in temperature. Most places where this system will be used, the temperatures will be around 4 - 6 degrees Celsius. Since the batch size is increased, this simplification makes the experiment more practical.

Experiment 3, like experiment 1, is a quantitative experiment. Figure 3.3 shows the form used to register the measurements for experiment 3. Note that this form has a column for temperature alongside the measurement column.

The figure displays nine identical data entry forms arranged in a 3x3 grid. Each form is a table with the following structure:

Date:	RPM	Temp	Measurement
$\theta_1$			
$\theta_{ao}$			
$\theta_{ao}$			
$\theta_a$			
$\theta_{ao}$			
$\theta_{ao}$			

**Figure 3.3:** Form used for experiment 3.

As in experiment 1, steps should be taken to ensure that the measurements are as accurate as possible.

### 3.3.4 Experiment 4 - Spacer Liquid Performance

The objective of this experiment is to investigate the spacer liquid’s ability to keep the production chemicals separate during operation of the system. This is experiment will therefore address research objective 2.a. To investigate this, a rig is built which will simulate transport in a pipe. There are several factors which can impact the spacer liquid’s ability to keep the production chemicals separate. The length of the spacer liquid pill, viscosity of the spacer liquid, length of transport, and flow-rate will affect the spacer liquid integrity.

This experiment will therefore have a certain degree of trial and error in the beginning. From the interviews, there are some indications that might give a starting point as to the length of the spacer liquid pill. Calculations can be done where the system design is taken into consideration with regards to viscosity of the spacer liquid.

Experiment 4 is a quantitative experiment. Just like experiment 2, visual measurements are used. A rope is used to measure the length of a liquid phase inside a tube. But, it can be hard to see where the phases start and end, and the measurements here will therefore be approximations. Figure 3.4 shows the form used in experiment 4.

Date	Notes
Gel length measured start	
Gel length measured end	
Time position 1	
Time position 2	
L position 1 to 2	

**Figure 3.4:** Form used in experiment 4.

Since this experiment is based on visual observations and approximate measurements, there is a field for notes. Here everything that might be relevant in discussions, but not apparent from the measurements, will be noted. Total run time was also noted in this field.

## 3.4 Equipment Used in This Thesis

### 3.4.1 Fann Viscometer Model 35SA

In this project, viscosity was measured using a Fann Viscometer, model 35SA. The information in this section is collected from the manual for the viscometer (Fann Instrument Company, 2016b).

The Fann viscometer is a direct reading rotational viscometer, meaning that the viscosity is directly indicated. By rotating a hollow cylinder, the rotor sleeve, around another coaxially placed cylinder, the bob, Couette flow is induced. This flow exerts a force on the bob which is measured by allowing the bob to rotate. A spring works to hold the bob in place. By knowing the force needed by the spring to hold the bob still at different rotational positions, the force from the Couette flow on the bob is measured. The force is proportional to the viscosity.

The spring, rotor sleeve, and bob may be changed to measure viscosities at different ranges, smaller or larger samples and at different temperatures. The standard configuration is known as R1-B1-F1, where R1 is the rotor sleeve, B1 is the bob, and F1 is the spring. Using the equation below, the viscosity is calculated from the measured apparent viscosity.

$$\mu = S * \theta * f * C \quad (3.1)$$

Here,  $S$  is speed factor,  $f$  is spring factor,  $C$  is rotor-bob factor, and  $\theta$  is the dial reading. The factors are given in tables A.3 and A.2 in appendix. Figure 3.5 shows a sketch of the Fann Viscometer.

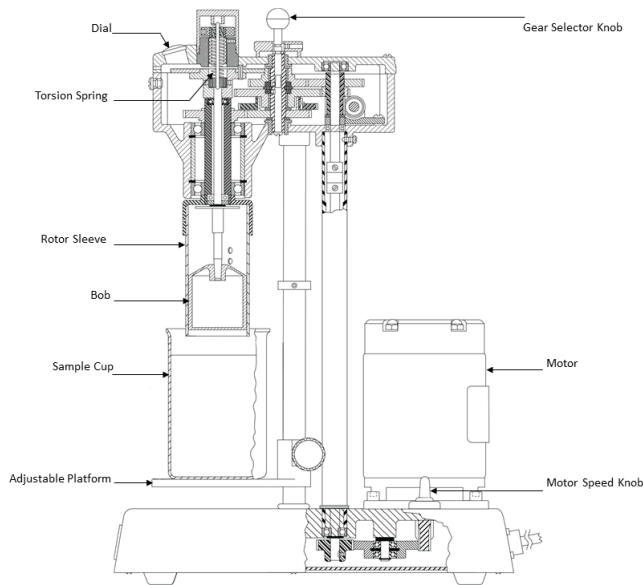


**Figure 3.5:** Fann Viscometer.

### Use

The Fann viscometer has six speeds. They are accessed using the two-speed motor and the three-position gear selector knob. The shear force is read from the dial.

The gel samples measured in this thesis would sometimes contain bubbles. The value displayed by the dial was unstable when the sample contained bubbles, but it seemed to stabilize if the viscometer ran a while before reading the dial. Thus, for all samples the viscometer ran for five minutes at the lowest speed before the measurements were taken.

Table 3.1 shows the different settings for the different speeds. The measurements were taken by toggling between the gears at the same speed, starting with the lowest gear and lowest speed. The order becomes 3, 100, 300, 6, 200, and 600 RPM.

RPM	Motor Speed Knob Setting	Gear Selector Position
600	High	Down
300	Low	Down
200	High	Up
100	Low	Up
6	High	Center
3	Low	Center

**Table 3.1:** Fann Viscometer Speed Settings.



### 3.4.2 Hamilton Beach Mixer

The Hamilton Beach HMD 200 is a commercial drink mixer (Hamilton Beach Commercial, 2018), but is also used as a high shear mixer for drilling fluids (Fann Instrument Company, 2018). It has a 1/3 horsepower motor and three speed settings.

#### Use

The mixer has a limited volume capacity for mixing. The cup can hold 500ml without spilling over during mixing. Mixing in this thesis is therefore done batches of 500ml. Where batches larger than this is necessary, 500ml is mixed at a time, then the 500ml batches are mixed together by hand. This is to ensure that the batches are equal with regards to lumping and to remove differences due to inaccuracies in measuring out and adding the powder.

### 3.4.3 Baroid Mud Balance

A mud balance is used to measure the density of a fluid. This section describes the mud balance used to measure density for this thesis. The information in this section is collected from the manual for the mud balance (Fann Instrument Company, 2016a). The Baroid mud balance from Fann consists of a cup with a lid connected to a balance arm. On the other side of the balance arm is a small compartment. This is filled with lead shots, and calibration is done by removing/adding lead shots. On the balance arm near the cup there is a knife-edge. Above the knife-edge there is spirit level. When measuring, the knife edge is placed on a fulcrum on a base stand. By moving a rider along the balance arm until the balance arm is level, the density is measured. The Fann mud balance can show density in four units. On one side the density is indicated in pounds per cubic feet ( $lbs/cu.ft$ ) and specific gravity ( $g/cm^3$ ), and on the other side in pounds per gallon ( $lb/gal$ ) and pounds per square inch per 1000 feet depth ( $lbs/sq.in/1000.ft$ ). Figure 3.6 show the mud balance used for this thesis.



**Figure 3.6:** Baroid Mud Balance.

#### Use

The mud lab contains two mud balances. To ensure uniformity in results, the same balance is used for all measurements.

The fluid to be measured is added to the cup. The cup should be filled almost to the rim. The cap is placed on the cup and gently pressed down until it rests on the cup. Spillage from the sides and the hole on top is removed with a paper towel. The knife-edge is placed on the stand as shown in figure 3.6. The rider is moved until the bubble in the spirit level remains stable within the lines. Where to read the result is indicated by an arrow on the rider.

### 3.4.4 Sartorius Quintix Model 224

The Sartorius Quintix Model 224 is a laboratory balance used in this thesis for weighing. It reads down to 0.1 milligrams and has a maximum capacity of 220 grams (Sartorius, 2017).

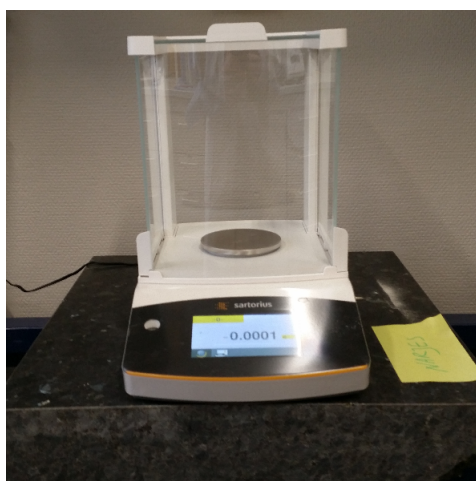


**Figure 3.7:** Sartorius Quintix Model 224.

#### Use

The balance is turned on by pressing the on-off button. The balance needs a few seconds before it is ready for use. When the displayed weight is stabilized and the balance is ready for use, the writing switches from gray to black. If a vessel is used, the empty vessel is now placed on the balance. Then the TARE-button is pressed. When the balance is ready again and stabilized at 0, the writing turns from grey to black. The object to weighed can now be loaded. To get the most accurate results, the door of the glass cage is closed. The writing turns from gray to black when the measurement is stable.

### 3.4.5 LabVIEW

An instrument is a device used to measure physical values and store or display these values. A virtual instrument, or VI, is a software application which gathers information from an instrument and handles the data by either performing operations or displaying them at the

computer. LabVIEW is a virtual instrumentation software platform. The name is short for *Laboratory Virtual Instrumentation Engineering Workbench*. It provides a graphical programming environment for the creation of VIs (Sumathi, 2007).

A LabVIEW VI has three main components: The front panel, the block diagram, and the icon and connector pane. The front panel is used for user interaction during operation of the VI. It makes controllers for input and indicators for display available to the user. The block diagram contains the graphical programming part. Figure 3.8 shows the front panel and block diagram for the valve control VI used in this project. A detailed description of the programming for the valve control can be found in the appendix, section C.

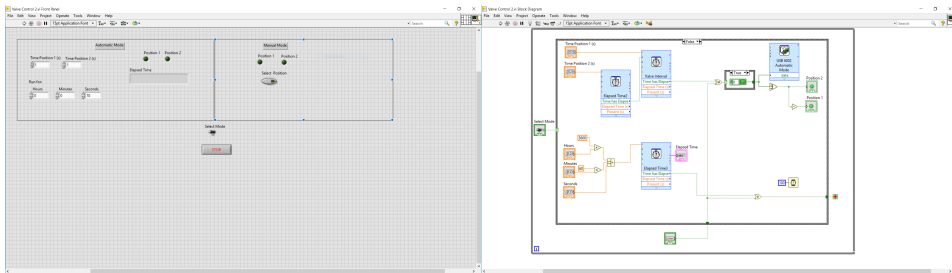


**Figure 3.8:** Left: Front panel of valve control. Right: Block diagram of valve control.



# Experimental Work

This chapter will outline the work performed at the mud-lab and in the laboratory hall at the Department of Geoscience and Petroleum Technology(IGP), and the process of identifying a spacer fluid. The results from the experiments are presented in chapter 5.

## 4.1 Deciding on Separator Liquid

In the oil and gas industry, gel pigs are very common. They are used for a range of purposes, and for the goal of this thesis, looking into gel pigs seemed to be the place to start. Several companies that produce gel pigs were contacted, and one replied. The representative of this company said polymers were often used for gel pigs, and there had been some previous experimental work where polymer gels were used as separator pills for jet fuel. However, he did not go into specifics about which polymers were used due to industry secrets.

An associate professor at the Department of Chemical Engineering at NTNU and expert in polymer technology was contacted. A short outline of the purpose of the thesis was presented to him. From the information provided, he proposed three possible candidates he thought might suit our purposes:

- Xanthan gum
- Scleroglucan
- Polyacrylamide

The staff engineer at the mud laboratory, Roger Overå was contacted and asked to provide input to the spacer liquid selection. Of the three candidates proposed by the associate professor, Roger Overå was most familiar with Xanthan gum. He also had a batch of XG powder on hand which was available for us to use. XG is non-toxic and already in use in the oil and gas industry as a viscosifier. Xanthan gum was therefore chosen as the first candidate for further research.

## 4.2 Experiment 1 - Viscosity and Density Over Time

In the proposed system, the production chemicals will spend some time in a pipe at the seafloor. Thus, they will get exposed to temperatures at the sea-bottom. It is therefore important to know how XGs rheology-characteristics will change over time when exposed to lower temperatures.

Equipment used:

- Fann Viscometer Model 35SA
- Baroid Mud Balance
- Hamilton Beach HMD 200
- Sartorius Quintix Model 224 Balance

### 4.2.1 Approach

#### Preparation of Xanthan Gum Gel

The viscosity of different concentrations of the XG gel was not known. It was decided to start with concentrations of 0.5wt%, 1wt%, and 1.5wt%. The viscosity measurements from this experiment were used in combination with information on the system from the thesis of Magnus Lund-Tønnesen to decide the concentration of the gel used in experiment 4.

500 grams of water was measured out. This was the maximum amount of water which could be mixed at a time in the Hamilton Beach mixer. The amount of Xanthan gum powder in grams was calculated using equation 4.1, solving for  $mass_{XG}$ . This results in approximately 500 ml of solution.

$$(mass_{water} + mass_{XG}) * \frac{wt\%}{100} = mass_{XG} \quad (4.1)$$

This step was repeated in order to get 1000 ml solution of each chosen concentration. The two 500 ml batches of each concentration were then mixed together by hand in order to minimize any differences in the samples. 500 ml of each concentration was put into cold storage, and the remaining solution was put in storage at room temperature.

#### Viscosity Measurements

Viscosity was measured initially after mixing, then three times a week (Monday, Wednesday and Friday). A Fann Model 35SA viscometer was used for viscosity measuring. 350 ml of the sample was poured into the sample cup, and tests were run according to the manual instructions. The result was noted in the form shown in figure 3.2 and later entered into an Excel workbook where the viscosity was calculated using equation 3.1.

Three batches of 1000 ml were prepared as described above. The viscosity and density of each batch were measured after preparation. Then, 500 ml of each batch were put in cold storage. The rest were put in room temperature storage. Viscosity was measured three times a week, and the density once a week. The reason the measurement frequency

is limited is due to loss of sample during measurements. It proved to be near impossible to get all XG gel back into their containers after testing, and the samples decreased with each measurement.

### Density Measurements

The density was measured for all samples at the day of preparation. For the rest of the experiment it was measured on the last day of viscosity measurements of the week, Friday. Density was measured using the Baroid mud balance and following the routines outlined in section 3.4.3.

This process was only performed for a limited amount of times because the measuring causes such a great loss of sample. It is important to remove all of the overflowing gel, and it was hard to collect this gel back into the storage vessel. A lot of the gel therefore had to be dried off using paper towels, and this causes the increased sample loss.

## 4.3 Experiment 2 - Chemical Compatibility

The XG gel will be exposed to several chemicals when used in the system. Experiment 2 was designed to investigate how the XG gel will react when exposed to the different chemicals it might be exposed to during use as a spacer fluid.

Equipment used:

- Hamilton Beach HMD 200

### 4.3.1 Acquiring Chemicals

In order to perform experiment 2, production chemicals are needed. Several companies who supply production chemicals were contacted and asked to help by supplying chemicals for the work in this thesis. The companies who were contacted will not be named in this thesis to ensure that no misunderstandings or offense occur. The companies who replied were guaranteed anonymity to ensure that no company secrets are revealed.

It took a long time to get replies from the companies, and most did not reply. Near the end of the semester, a connection was established with a well known chemical supplier in the oil and gas industry. They sent us samples of a corrosion inhibitor, a biocide, and a demulsifier. However, it turned out the chemicals we were sent were actually meant for mixing into drilling mud and not for injection into the production stream. Research was done in order to see if it was possible to use the chemicals we were sent, but the answer was not found.

We were able to acquire ethylene glycol, which is a common anti-freeze. For this thesis, ethylene glycol is referred to as glycol for simplicity. This was used to represent MEG, a common hydrate inhibitor. The reasoning was that MEG is chemically similar to glycol. The chemical compatibility between the spacer liquid and glycol will give an indication to the chemical compatibility between the spacer liquid and MEG.

### 4.3.2 Approach

Three 100 ml batches of 0.5 wt%, 1.0 wt%, and 1.5 wt% XG gel respectively were mixed using the Hamilton Beach mixer. They were put into 250 ml flasks with 100 ml of each chemical they were tested against. Initial reactions were noted, and pictures were taken. The batches were put into storage and new pictures were taken every day the first week, then once a week for the following weeks. This shows how much the gel has dissolved, or if any other reaction has occurred.

#### Hypothesis

1. The viscosity of the cold sample will be higher than the viscosity of the room temperature sample.
2. The viscosity of both samples will not change over time.
3. The density will not change over time.

The reasoning behind the first hypothesis is that for most liquids viscosity increases when the temperature drops. If the storage vessel is airtight, there is no reason to believe that there will be a change in viscosity over time as water will not evaporate away and increase the XG concentration. However, some water may evaporate during testing. This might increase the viscosity. But it is not believed that this will happen to a degree that will change the viscosity noticeably. Therefore, the second hypothesis is that the viscosity will be stable over time. For the same reasons as mentioned for the second hypothesis, it is believed that the density will not change over time.

## 4.4 Experiment 3 - Viscosity and Density Over Time - Extended

From experiment 1, it was found that 0.5wt% XG seemed like the most reasonable concentration. Experiment 3 would therefore only consider 0.5wt% XG gel. Experiment 3 tests how the 0.5wt% XG gel's viscosity evolves over time at reduced temperatures when not exposed to air.

Equipment used:

- Fann Viscometer Model 35SA
- Baroid Mud Balance
- Hamilton Beach HMD 200

10 samples of 500 ml 0.5wt% XG gel were prepared. They were mixed together to create one batch, then split back into 10 samples. One sample was tested right after mixing, the rest were put into cold storage.



### 4.4.1 Viscosity Measurements

Once a week, a fresh sample was taken from cold storage and the viscosity was measured. Viscosity was measured just like in experiment 1, but the temperature was measured simultaneously and registered for each viscosity measurement. Figure 4.1 shows the set-up for viscosity measurements with temperature measurement. Using the edge of the viscometer to support the thermometer as shown in figure 4.1 was done to ensure that the temperature measurements were taken consistently.



**Figure 4.1:** Setup for viscosity measurements

The viscometer reading and temperature were noted in the form shown in figure 3.3, and subsequently entered into an Excel document. The viscometer readings were converted to viscosity in the Excel document, and statistical analysis was performed on the results.

### 4.4.2 Density

Since the samples are not going to be re-tested, density measurements were taken as often as the viscosity measurements, once a week. This was done using the Baroid Mud Balance as described in experiment 1.

## 4.5 Experiment 4 - Spacer Liquid Performance

Experiment 4 was conducted in the Hall Laboratory at IGP. The objective of experiment 4 is to investigate the ability of a potential separator fluid to keep the chemicals separated during operation. Several approaches were considered.

First, it was proposed to lay tubing around an existing copper-pipe construction in the laboratory hall. From the preparatory work done during the specialization project in the preceding semester, it was found that a pipe with a diameter of 0.5 inches would be sufficient for the system. It was then calculated that a tube with an inner diameter of 0.5 inches laid tightly around the copper-pipe construction would give a total pipe length of 500 - 600 meters. However, this plan was abandoned as it would be a significant investment with no guarantee of effectiveness.

A smaller build was proposed. Here, the chemicals would be in a u-shaped tube and be pushed back and forth. Mechanical movement of the tube was the first idea for inducing flow. However, there were concerns that due to the viscosity of the gel, the liquids would not flow in this configuration. Application of pressurized air to propel the liquids was proposed and decided on. A pneumatic directional solenoid valve was chosen, and a LabVIEW virtual instrument was programmed for control of the valve. This valve alternates the side at which pressure is applied. The inner diameter of the tube was set to 10mm, following new calculations performed by Magnus Lund-Tønnesen in his thesis. A clear PVC tube was chosen due to its chemical resistance properties and its transparency. Figure 4.2 shows the test set-up.

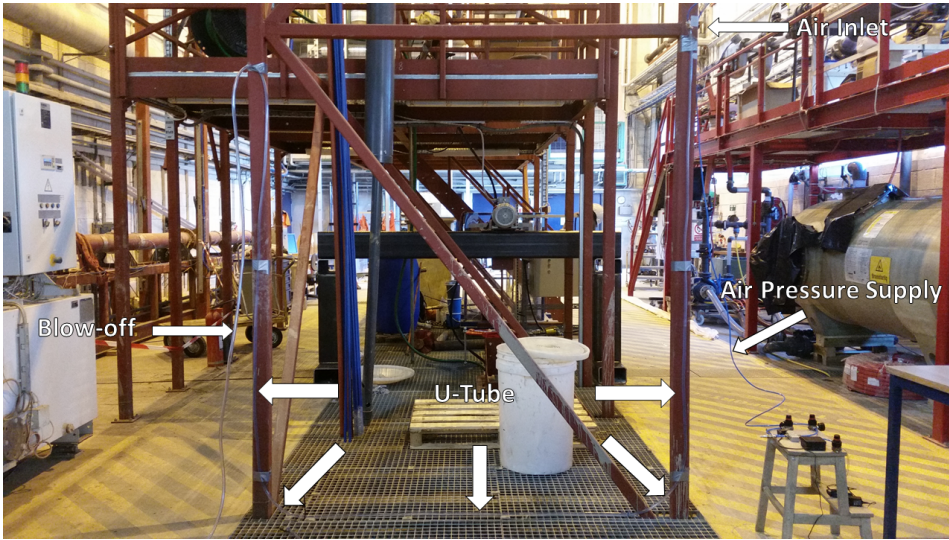


**Figure 4.2:** Experiment 4 test set-up.

The amount of gel needed depend on the length of gel pill wanted, and is calculated using equation 4.2.

$$V_{gel} = \frac{\pi * d^2}{4} * l_{gel} \quad (4.2)$$

Here,  $V$  is the volume of gel in liters,  $d$  is diameter of the pipe in meters, and  $l_{gel}$  is the wanted length of gel pill in meters. The expert on gel pigs that were contacted at the start of the project had suggested that a gel length of 5 to 10 meters would be sufficient for transport lengths of 10 to 30 kilometers. We assumed that 5 meters of gel pig would be enough for the initial runs. There was some loss of gel during loading, which leads to the actual gel pill length being shorter than the calculated one. The actual length was therefore measured using a rope along the outside of the tube before start.

Pressurized air is connected to the intake of the solenoid valve, and the LabVIEW VI alternates the pressure on each side. The travel length,  $L$ , is measured as shown in figure 4.3.

The run-time is set before starting the experiment, and time in each position of the piston is set. Equation for total simulated transport length,  $L_{TS}$ , is shown in equation 4.3.

$$L_{TS} = \left( \frac{t_{total}}{t_{pos1} + t_{pos2}} \right) * 2L \quad (4.3)$$

Here  $t_{pos1}$  and  $t_{pos2}$  is the time spent in valve position 1 and 2 respectively. The flow velocity is calculated according to equation 4.4.

$$v = \frac{2L}{t_{pos1} + t_{pos2}} \quad (4.4)$$

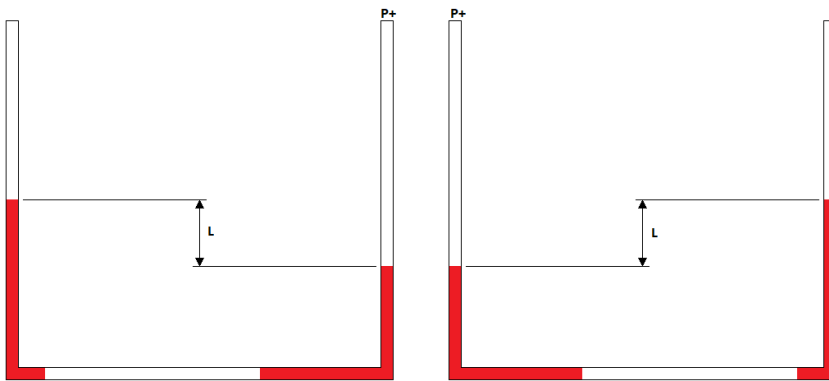


**Figure 4.3:** Model showing travel length  $L$  for the test loop

After the experiment has run for the designated time, the observable length of the gel is measured again using a rope along the outside of the tube.

It proved difficult to load the gel and chemical into the pipe without trapping air or mixing the chemical and gel. A device was built to ease loading. It consisted of two funnels leading into a three-way ball valve with an L-bore, as shown in figure 4.4. Here, gel is loaded on one side and chemical in the other while the valve is in the closed position. The device is moved and attached to one end of the tube. The valve is moved so the chemical loads, and when the appropriate amount is loaded into the tube, the valve is switched so the gel loads. When the gel is finished loading, the valve is switched back so the rest of the chemical is loaded. This solution was designed with a ball valve with an L-bore. But when the order arrived, it was a ball valve with a T-bore. To save time it was tried using the T-bore valve, but this was not efficient.

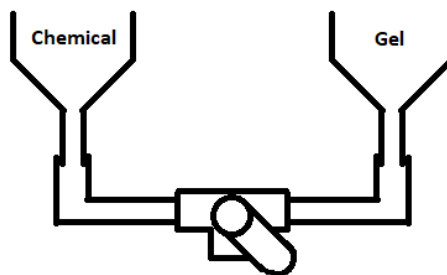


**Figure 4.4:** Loading device.

The final solution was to load the gel into the tube first and manipulate the tube to get the gel into place. Figure 4.5 show the loading procedure.

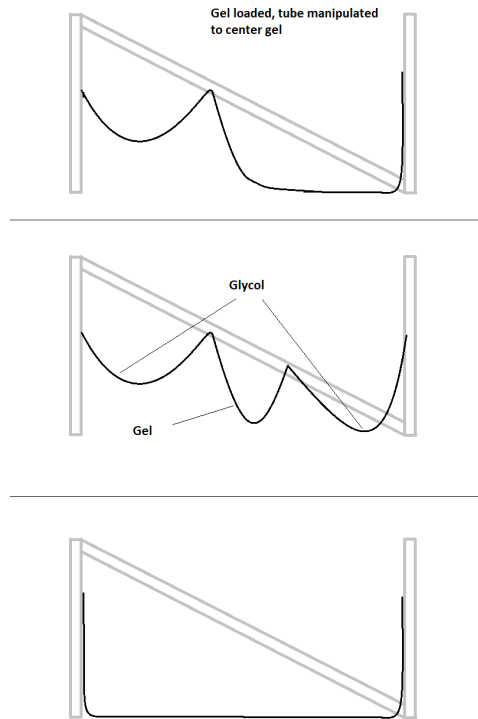


**Figure 4.5:** Loading Procedure

The gel is loaded into the tube while the tube is in the top position of figure 4.5. The right side of the tube is lifted so that the gel gathers towards the center of the tube. When the gel is centered, the tube is attached to the metal beam as shown in the middle part of figure 4.5. Then glycol is loaded into each side. When all the glycol is loaded, the tube is lowered into the position shown in the bottom of figure 4.5. This proved to be the most efficient loading procedure and resulted in minimal mixing before start.

### 4.5.1 Modifications

As shown in chapter 5, at gel pill lengths up to 5 meters, the gel seems to mix too much with the glycol. It was decided to increase the concentration of the XG gel, and to increase the length of the tube to allow for longer  $L$  and  $l_{gel}$ .

#### Increased Xanthan Gum Concentration

This modification was implemented to see if the higher viscosity of a more concentrated XG gel would help keep the chemicals separate. One batch of 0.75wt% XG gel and one batch 1wt% XG gel was prepared. The experiment was repeated as before. The batches

were sized so that they would be enough for a total of 10 meters in the 10mm tube. Two runs were performed with each gel and with a gel pill length of approximately 5 meters. These runs were exploratory runs to see if there would be an immediate difference when the viscosity was increased.

### Longer Tube

This modification was implemented to see if a less frequent change of flow direction would result in less mixing. The type of tube is the same as the one used earlier.

A simple model of the first setup is shown in figure 4.6. However, when pressure was applied in this configuration, the liquids would settle in the bottom of the tube and the air would bubble through.

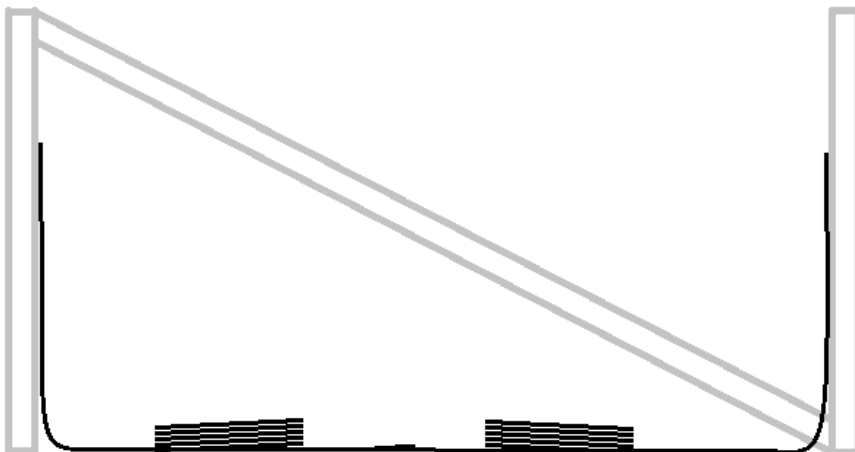


**Figure 4.6:** The first 100-meter solution

A second design for the 100-meter solution was tried. A model of the new design is shown in figure 4.7.

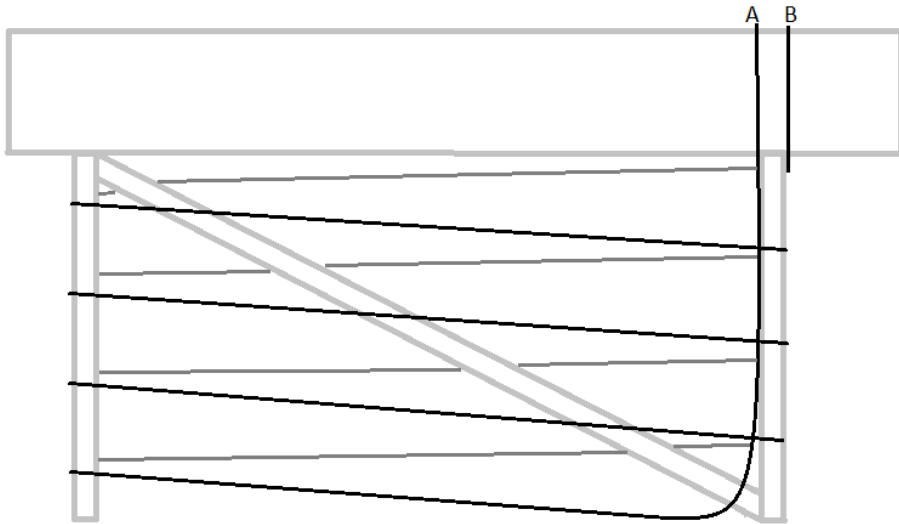


**Figure 4.7:** Second 100-meter solution

Here the tube was wound around four beams. On top of the beams is a platform. The liquids were loaded from this platform. Gel was first loaded into end A. Then glycol was loaded into end A and B. This resulted in a gel pill with glycol on either end. It proved difficult to get enough incline in this configuration to overcome the sag between connection points. When the liquids were loaded into the tube, the tube started to sag between connection points. The liquids settled in these sags, and the air bubbled through rather than push the liquids.

To increase the incline the length was reduced to 50 meters. In this configuration, the air started to bubble through the liquids when the air reached the bottom of the tube. However, unlike the previous configuration, it was now possible to push the liquids back up the vertical stretch by applying pressure into end B. The experiment was now carried out by pushing the liquid up and down the vertical stretch. This left most of the tube unused, but the  $L$  was increased compared to the configuration shown in figure 4.2.





# Results

## 5.1 Experiment 1 - Viscosity and Density Over Time

### 5.1.1 Viscosity Measurements

Experiment one ended earlier than anticipated. A small amount of the sample was lost each time the tests were conducted. After about a month the samples were close to the minimum amount needed for viscosity measurements. Test frequency was reduced from three times a week to once a week. But now the 0.5wt% samples started showing signs of mold. The sample was no longer usable, and the experiment was discontinued. A new experiment, experiment 3, was designed with the problems of experiment 1 in mind.

Xanthan Gum is a pseudoplastic liquid (Sworn, 2009), and the tests confirm this. As figure 5.1 shows, the viscosity of 0.5wt% decreases as shear rate is increased. This behaviour was found for all samples, and matches the viscosity plot for pseudoplastic liquids shown in figure 2.7. Tables with results for all samples are found in the appendix.

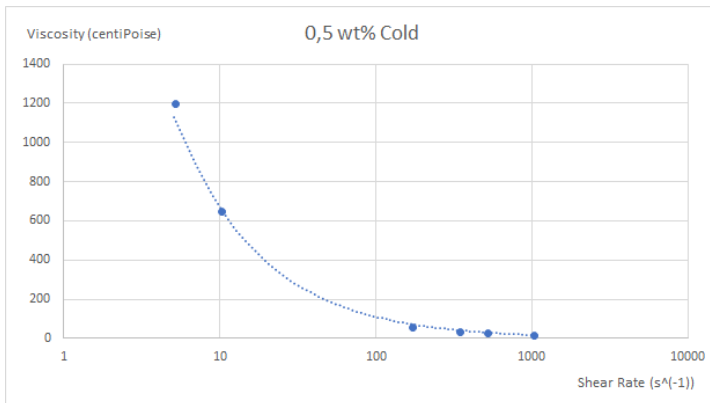


**Figure 5.1:** Viscosity at different shear rates

Figures 5.2 and 5.3 show the measured viscosity for the 1.5wt% XG gel. At lower shear rates the measured viscosity is highly variable, especially for the sample stored at room temperature. The measurements seem more stable at higher shear rates. For the other samples with different concentration there was less variation in the measurements. Tables for all samples at all shear rates can be found in the appendix.

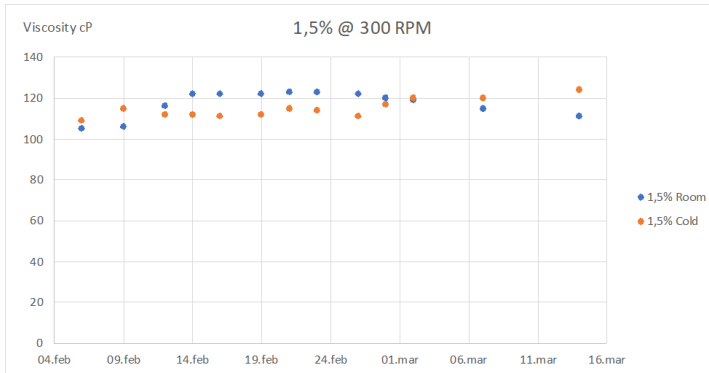


Figure 5.2: Viscosity over time at 300RPM,  $511s^{-1}$

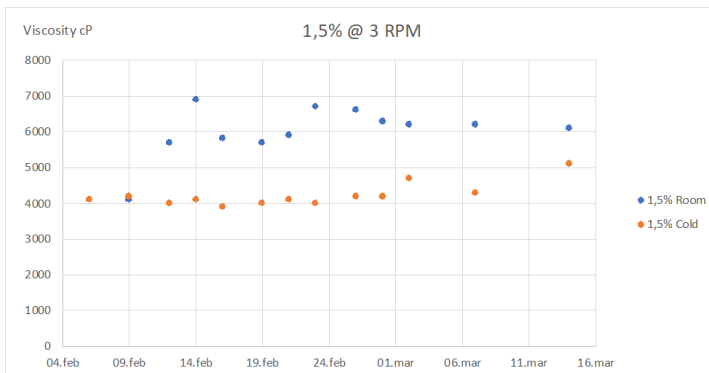
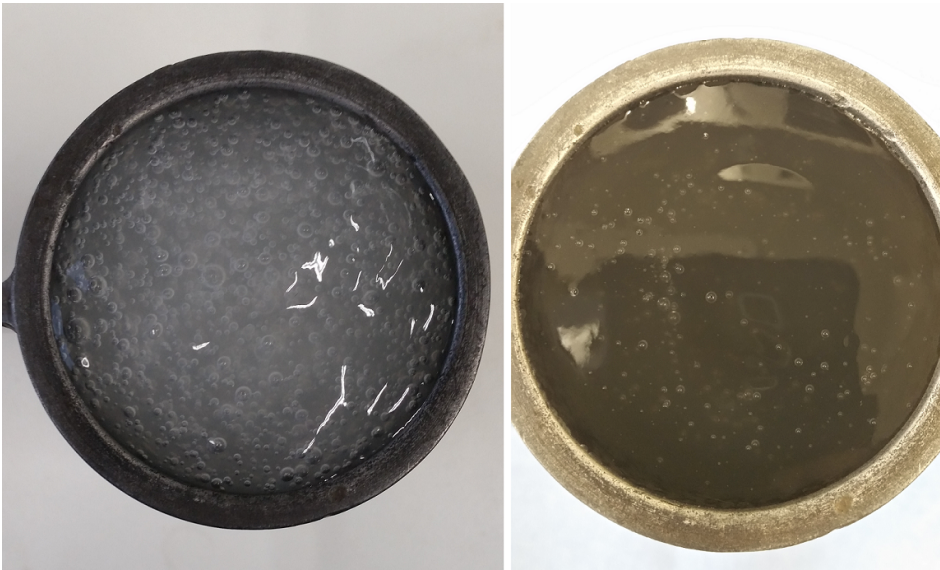


Figure 5.3: Viscosity over time at 3 RPM,  $5.1s^{-1}$

### 5.1.2 Density Measurements

The density of all samples ranged from  $0.96$  to  $0.98g/cm^3$  for the first measurements. The samples did however contain a significant number of bubbles. When the samples were more or less free of bubbles, the density of all but one sample were  $1g/cm^3$ . The results are shown in table B.7 in the appendix. Figure 5.4 shows how the bubbles developed in a sample with an XG concentration of 1wt% over two weeks. At the time of the left photo the sample showed a density of  $0.97g/cm^3$ . At the time of the right photo, the density measured was  $1g/cm^3$ . Therefore, it would seem as if the density increases over time, but it seems as if this is more because of a reduction in the number of bubbles.



**Figure 5.4:** Left: Bubbles right after mix. Right: Bubbles after two weeks.

### 5.1.3 Mold Development

After running experiment 1 for a little over one month, the sample sizes had reduced considerably due to losses when re-bottling the samples after testing. At least 350 ml is required to do viscosity measurements in a Fann viscometer. It was decided to reduce the frequency of testing to once a week in order to limit the sample loss. However, some samples started to show signs of mold formation, as shown in figure 5.5. The lower concentration samples, 0.5wt% and 1wt% were the samples which were affected. The worst was 0.5wt% stored at room temperature.

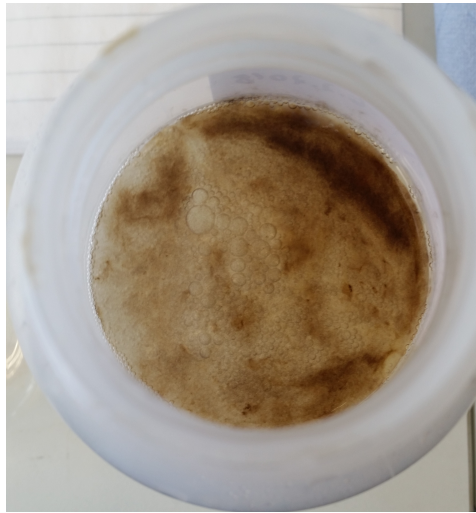


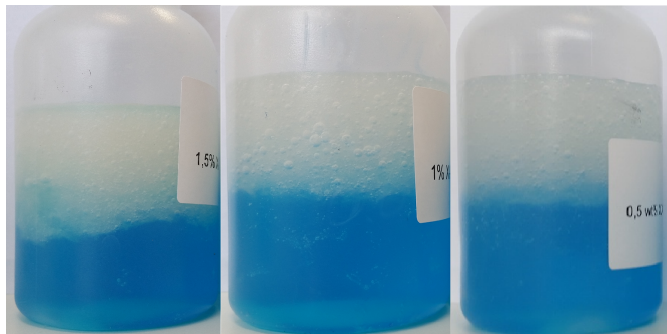
**Figure 5.5:** Mold in sample

With some samples being spoiled, it was decided to abandon experiment 1, and start a new experiment, experiment 3, with a new approach.

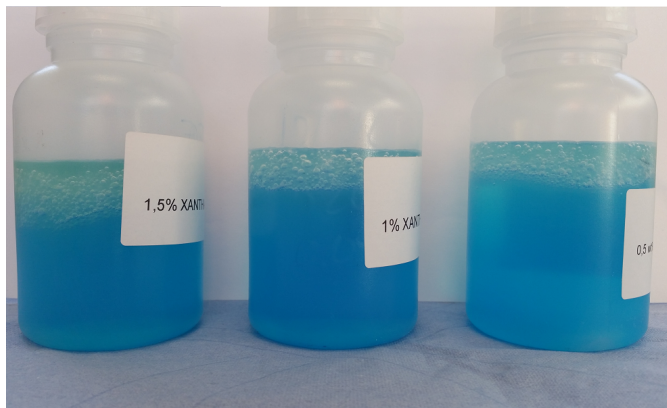
## 5.2 Experiment 2 - Chemical Compatibility

Figure 5.6 shows bottles containing 100 ml gel and 100 ml glycol on the day of mixing. Figure 5.7 shows the same bottles after seven days. For all concentration XG gels, the glycol seemed to not dissolve much gel right after mixing. The gel settled on top, which is in line with the density of the gel with bubbles seem to sit around  $0.97$  to  $0.98 \text{ g/cm}^3$ , and the density of glycol being about  $1.1 \text{ g/cm}^3$ .

After a week, all the mixes had stabilized. It seems to be the case that the higher concentration gels have dissolved less. But, the low concentration gel seems to have dissolved less over the week, with most of the dissolution happening right after initial mixing. Pictures from 0, 7, and 30 days after mixing gel with glycol are found in figures B.7 to B.9 in the appendix.



**Figure 5.6:** Bottles with 100ml gel and 100ml glycol. From left to right: 1.5wt%, 1wt%, 0.5wt%



**Figure 5.7:** Bottles with 100ml gel and 100ml glycol. From left to right: 1.5wt%, 1wt%, 0.5wt%

### 5.3 Experiment 3 - Viscosity and Density Over Time - Extended

There was no sign of mold development when only testing the samples once and limiting the air in the flasks. The viscosity measurements seem consistent with the results from experiment 1. Using Microsoft Excel to perform a t-test with equal variance in Excel to compare the results of the 0.5wt cold sample in experiment 1 with the measurements from experiment 3, we see that for half of the shear rate groups the average is significantly different. We are assuming equal variance as the equipment used is the same and the measurements are performed at the same place under very similar conditions. Tables with all the results are given in section B.3 in the appendix.

Figure 5.8 shows results from experiment 3 and experiment 1 at  $170s^{-1}$ . According to the t-test, the average value of these results is significantly different. Visually, however, they appear to be very similar. Figure 5.9 shows the same plot but at  $511s^{-1}$ . According to the t-test, these results do not have a significantly different mean.

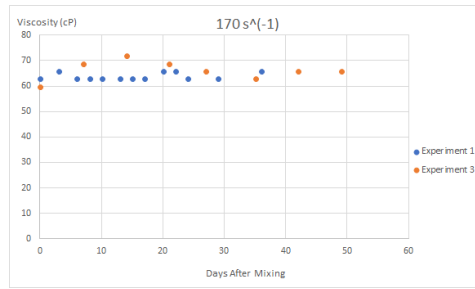


**Figure 5.8:** Viscosity measurements from experiments 1 and 3 at  $170\text{s}^{-1}$ .

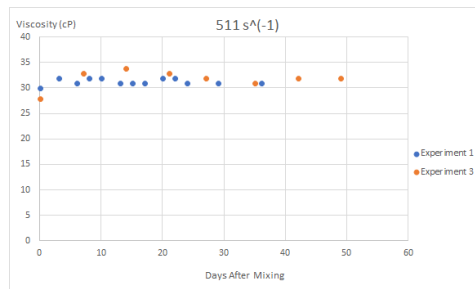


**Figure 5.9:** Viscosity measurements from experiments 1 and 3 at  $511\text{s}^{-1}$ .

Like in experiment 1, the density seemed to follow the number of bubbles, and the number of bubbles decreased over time. Therefore, it is hard to separate the effect of time on density from the effect of bubbles on density.

## 5.4 Experiment 4 - Spacer Fluid Performance

The first run with glycol and XG gel was cut short due to trouble during start-up, so the experiment only ran for 2 hours with a simulated travel-length of 96m. It was hard to see any explicit divide between the gel and the glycol after the run, so measurement of the length is only an approximation. Figure 5.10 shows the transition between gel and glycol before and after the 2-hour run.

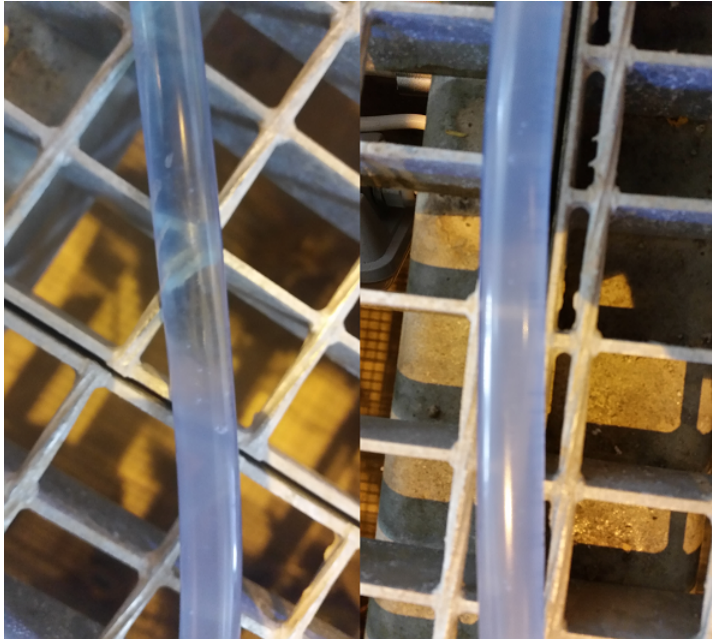


**Figure 5.10:** Left: Gel-Glycol transition before run. Right: Gel-Glycol transition after run.

It is a much less clear transition on the after picture on the right hand side, but it is still mostly cloudy white at the bottom and blue at the top. The gel is the cloudy white phase, and the glycol is blue.

For a run-time of two hours, a 20% reduction in gel pill length was observed. However, for run-times of 4 hours or more, independent of the length of gel pill, there seemed to occur mixing across the full length of the gel pill. In disposal of the chemicals after the experiment, it was observed a higher viscosity when the content at the center of the tube was drained, but it was clearly colored blue from the glycol. Table 5.1 shows the run times and gel lengths for the initial runs. A full table with all variables from these runs is shown in figure B.12 in the appendix.

Run Time (hr)	Gel Pill Start Length (m)	Gel Pill End Length (m)
2	3.5	2.8
4	3.4	0
5	4.6	0
5	4.9	0

**Table 5.1:** Results from initial runs of experiment 4.

Experiment 4 had more runs than what is shown in table 5.1 and figure B.12. But there was a problem with the USB interface used to control the pneumatic directional valve. The computer would sometimes lose the connection with the interface, and the valve would be stuck in one position. If it was left in one position long enough, the liquids were pushed



too far up and into the pneumatic portion of the system. These runs were then aborted, and the equipment had to be cleaned. However, the results from the concluded runs are quite clear, and more runs feel excessive.

In addition to the mixing of the gel and glycol, there was also observed some migration of the gel. It seemed the gel would get break into smaller pieces which would shift toward the highest points due to the difference in density. Figure 5.11 shows the two ends of the tube. A small amount of gel is observed on the left side, but a significant portion of the gel has migrated to the right end.



**Figure 5.11:** Gel migration

Three possible reasons for the mixing and migration were identified. The first was the viscosity of the gel, the second was the frequent change in flow direction, and the third was the length of the gel pill. The experiment was therefore modified to investigate this. Firstly, the experiment was performed again with a higher XG concentration gel. This will increase the viscosity. Secondly, the experiment was performed with 0.5wt% XG gel, but with an increased tube length. This allows for a longer travel before the flow direction is reversed and a longer gel pill.

## **5.4.1 Results From Modified Runs**

### **Increased Xanthan Gum Concentration**

Increasing the viscosity did not seem to help. Mixing and migration of the gel to the ends of the loop were still observed. Two runs were done with the 0.75wt% XG gel, and two



runs were done with the 1wt% XG gel. The results from these runs are shown in figure B.13.

### Increased Tube-length

Increasing the tube length allowed for a longer gel pill as well as a longer travel before the flow direction was reversed. Increasing the gel pill length did not help. Mixing of the gel and glycol was observed, as well as migration of a significant amount of the gel. Increasing the length travelled did not help. In a lot shorter span of time than with the shorter travel length, a significant amount of gel had migrated to the ends of the tube.

By the time the runs with increased length were tried, the semester was near the end and it was not time to do more runs.

### 5.4.2 Residue in Tube

Before using the rig, it was tested by running water through the tube. This resulted in some residue depositing inside the tube. Figure 5.12 shows the residue inside a piece of tube. The residue was not sticky, and disappeared easily when touched.

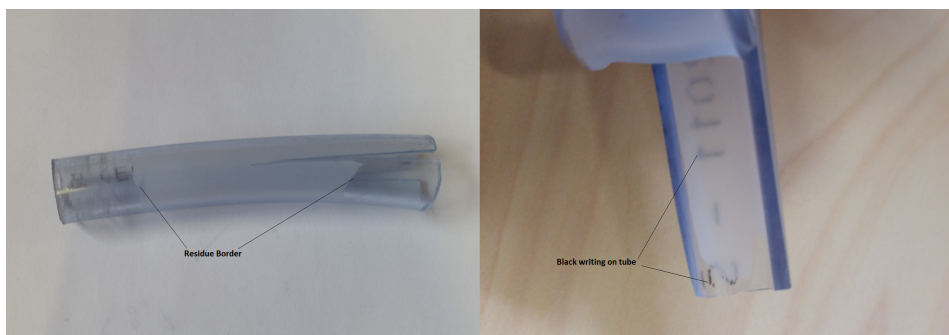


**Figure 5.12:** Left: Border of residue can be seen. Right: Black writing behind residue compared to black writing behind no residue.



## Discussion

This chapter discusses the results presented in the previous chapter and interprets them in relation to the objectives presented in section 1.2.

### 6.1 Experiment 1 - Viscosity Over Time

Tables B.1 to B.6 show the results for all viscosity measurements. It was hard to see any definitive change in viscosity over time for any of the samples. The measurements of the 1.5 wt% sample seemed very unstable, especially for the sample stored at room temperature. But there was not any readily apparent direction of change in the measurements.

There may be several reasons for the unstable results at the highest concentration XG mix. Polymer gels can be hard to mix as they are prone to lumping. Furthermore, if lumps are present it might be hard to see the lumps. If the gel contains lumps, the viscosity is not uniform across the sample. A Fann viscometer utilizes the Couette flow between a rotor and a bob to measure the viscosity. If one measurement is done with lumps between the rotor and the bob, the viscosity would register as higher than a measurement without lumps between the rotor and bob. The unstable measurements may therefore indicate a less efficient mix for the 1.5wt% sample. This sample was the first that was mixed. The pouring of the powder into the mixer required some technique to evenly distribute the powder. It may be that the pouring technique for this sample was not refined enough, and this sample contains more lumps.

A reason for the changes seen in viscosity could also be variations of temperature of the sample at the time of measurement. To investigate the relation between temperature and viscosity, correlation and regression analysis were performed. All tables with correlations between temperature and days after mixing can be found in the appendix in figures B.1 to B.6. They were made using the correlation data analysis tool in Excel, which calculates the Pearson correlation between each set of variables. The average correlation coefficient was found to be -0.309 for all viscosity measurements to temperature, and 0.110 for all viscosity measurements to days after mixing. However, the 1wt% and 0.5wt% samples stored at room temperature shows a negative correlation to days after mixing while the

other samples have a positive correlation here. Calculating the average of the absolute values gives an average correlation of 0.465 between viscosity and days after mixing.

These are relatively weak correlations. Using the table in figure A.1 with an alpha of 0.05 and N equal to 13, giving a df of 11, a correlation with an absolute value of 0.476 or above is necessary for the correlation to be considered significant.

Looking at the individual correlations, they range from -0.135 to -0.511 for temperature correlations, with two having an absolute value above 0.476. For time after mixing they range from 0.061 to 0.807. This range is for absolute values. Four of the 6 samples show an average correlation to days after mixing above 0.476. But 4 correlation coefficients are positive, and two are negative. It is hard to conclude anything from these results.

The weak correlation between viscosity and temperature is suspect, as it seems natural to assume viscosity varies with temperature. This is most likely due to a weakness in the design of the experiment. In this experiment temperature is measured once at the start, then viscosity is measured. This will not catch any development in temperature during viscosity measurements. Especially for the samples in cold storage, the temperature may vary significantly from the first measurement to the last. It was therefore decided that for the follow-up experiment, experiment 3, the temperature would be taken for every measurement. It is suspected that there will be a stronger correlation between the temperature and viscosity here.

## 6.2 Experiment 2 - Chemical Compatibility

The purpose of this experiment was to ensure that the spacer fluid under consideration was chemically compatible with the injection chemicals it will separate. However, finding suppliers who would provide us with samples of injection chemicals proved difficult. This may be due to fear that the chemicals will be tested in such a way that proprietary secrets are revealed.

Near the end of the project, however, we were able to acquire some samples of chemicals such as corrosion inhibitor, biocide and demulsifier. However, it turned out that the chemicals we got samples of were meant for mixing into drill fluid, and not for injection into the production stream. Inquiries were made in an effort to understand the difference between the chemicals we had samples of, and the chemicals used for injection. But we were not able to find a satisfying answer. Through Kelland (2014f) we were able to identify the chemicals we had samples of, and confirm that the same types of chemicals are used for chemical injection. However, the concentrations used and possible diluting agents are not identified. We were, therefore, not confident that we could make the chemicals representative enough for testing. Using these chemicals in experiments with the current knowledge would not yield valid results.

### 6.2.1 Exposure to Glycol

To represent MEG, a common hydrate inhibitor, we used ethylene glycol. This is a common antifreeze, and we were able to acquire this without contacting producers of production chemicals.

The XG gel seems to dissolve somewhat after mixing, but it seems to stabilize after a few days for all concentrations. There was seemingly no other reaction. The testing in this thesis did not estimate the amount of gel that dissolved. If XG gel is used as a spacer liquid, it will be necessary to establish the levels of dissolution. This should be done for all chemicals that are transported using this system so that the concentration of the chemicals that are injected are correct. Testing the levels of dissolution should perhaps be part of the evaluation performed by a chemical engineer when deciding the chemical injection regime.

### 6.3 Experiment 3 - Viscosity and Density Over Time - Extended

Table B.9 shows the adjusted  $R^2$ ,  $R^2$  to temperature and  $R^2$  to time for measurements at all shear rates for the results of experiment. A higher  $R^2$  indicates a stronger correlation. For all except 340.5 and 1021.4  $s^{-1}$ , the correlation increases from the adjusted  $R^2$  to  $R^2$ . This indicates that the correlation to time is weak, and this is confirmed when looking at  $R^2$  for time alone. A correlation between time and viscosity can therefore not be assumed.

Measuring the temperature for each viscosity measurement resulted in a very strong correlation coefficient, ranging from -0.81 to -0.96. This means higher temperature is related to lower viscosity, which is as expected. The correlation coefficient does not imply the magnitude of the temperatures impact on viscosity. Performing regression analysis on the results of this experiment at a shear rate of 170.23  $s^{-1}$ , we get the following equation for viscosity as a function of temperature.

$$\mu = 70.04 - 0.36T \quad (6.1)$$

Only the temperature is used in this equation as the analysis of correlation to time did not conclude that there is a significant correlation between viscosity and time. We used the results from the measurements at 170.23  $s^{-1}$  because this is closest to the shear rate in the pipe when we use a diameter of 10 mm and the flow velocity provided by Magnus Lund-Tønnesen from his work on the system side, 0.2 m/s. This is found using equation 2.2.

Using equation 6.1, the viscosity at different temperatures can be calculated. Table 6.1 shows the calculated viscosity for 20 and 4°C.

Temperature (°C)	Viscosity (cP)	Increase (Percentage)
20	62.8	0 %
4	68.6	9 %

**Table 6.1:** Calculated viscosities at different temperatures

A reduction of 16°C gives a 9% increase in viscosity. The temperatures chosen was chosen because fresh-water is at its most dense at 4°C. It is not the same for salt-water, but the density is dependent on the salinity of the water. So for simplicity we assume a seabed temperature of 4°C. This indicates that even though the correlation to temperature

is strong, the viscosity does not change very much when moving from room temperature to seabed temperature. Assuming 5 meters of gel spacer and 10 meters of each chemical, calculating the pressure drop due to friction, the difference is 37 bar over 30 km of pipe.

The density seemed to follow the number of bubbles in the sample rather than time or temperature. It ranges from  $0.96 \text{ g/cm}^3$  to  $1 \text{ g/cm}^3$ , and it was clear that the samples containing less bubbles were closer to  $1 \text{ g/cm}^3$ . A conclusion to whether density is stable over time or not is hard to reach due to the bubbles present. It was suggested that placing the samples in an environment with a pressure below ambient pressure would remove the bubbles faster. However, there was no equipment available to us at the time that could do this.

### **6.3.1 Comparing results to experiment 1**

Comparing the data sets from experiment 3 and experiment 1 with a t-test gives inconclusive results. However, the results from experiment 1 at 6 RPM are quite unusual. All measurements are the same. Therefore, there is an extremely large difference of averages here since the variance is very different. Therefore, the results from this t-test are not reliable. Also, the data sets are relatively small. A rule of thumb for t-tests is an N of at least 20. For experiment 3, especially, the number of measurements is very low. The results from the t-test in total are therefore not very reliable, and we cannot conclude whether the sets are equal.

However, we are measuring a gel that should have approximately the same XG concentration. They are stored in the same refrigerator and the measurements are performed with the same equipment. This indicates that there should not be any difference. And whether or not there is a difference, both experiment 1 and 3 shows that the viscosity does not change much over a time period of around 1.5 months. And it is unrealistic to assume that the chemicals will spend much longer than that in the pipe.

## **6.4 Experiment 4 - Spacer Fluid Performance**

### **6.4.1 Rigging**

Experiment 4 had a slow start. A design for the test rig needed to be decided, and the rig needed to be built. It was also necessary to get production chemicals to use for testing.

The first design proposed using an existing structure in the laboratory hall. A pipe would be attached to the outside of a copper pipe coil, and the gel and chemicals would be propelled by a pump. However, this limited the length we could simulate, as re-circulation through the pump would shear the chemicals and gel. This would give an unrealistic level of mixing. Using a smaller build that pushed the liquids back and forth would make it possible to simulate longer lengths than what was possible with this build. It would also be cheaper.

The next design had a tube shaped like a u where the ends of the tube would be moved up and down. The liquid inside would move back and forth relative to the tube due to the motion of the tube. However, in this solution there is a risk that the liquids would not move

if the friction from the liquids is too great for gravity to overcome. And if the liquids flow, the flow velocity cannot be controlled but rather be dependent on the friction.

The final solution was to use a u-tube, like the design proposed above, but to push the liquids with pressurized air. This solution was built using a 10m long see-through plastic hose with an inner diameter of 10mm. A Metalwork 5/2 pneumatic valve was used to distribute the air pressure, and it was controlled by a LabVIEW VI.

It proved difficult to load the liquids into the tube. If the liquids were loaded sequentially, air was trapped when the gel was loaded, as shown in figure 6.1.

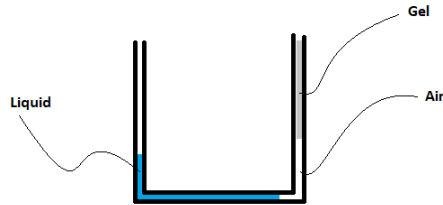


**Figure 6.1:** Air trapped in tube.

To deal with this, a device for loading was designed. But due to the wrong equipment being delivered, this device was abandoned. The final solution was manipulation of the device as discussed in section 4.5.

## 6.4.2 Running Experiment

For all run-times for 4 hours or more, it seemed as if the gel pill did not keep the chemicals completely separate. At the end of the run there were no distinct phases of gel and glycol, all the content of the tube was blue from the glycol. However, the content in the middle of the tube clearly had a higher viscosity than at the ends, indicating the gel mainly stayed in the center of the tube. But the gel was blue instead of cloudy white, indicating mixing with the glycol.

Four factors that might be crucial for the integrity of the pill were identified:

- Viscosity
- Flow rate
- Pill length
- Frequency of flow direction change

As observed in experiment 3, the viscosity of the gel is inversely related to temperature. Experiment 4 is conducted in a hall with an ambient temperature around  $20^{\circ}C$ . However, as discussed in 6.3, there is not a big difference in viscosity between 4 and  $20^{\circ}C$ . Even though this experiment is performed in an environment with an ambient temperature above the expected temperature of operation, there is no reason to suspect that the XG gel will

behave significantly different. Therefore, if the temperature is the reason for the inefficient gel pill, there is no reason to suspect the gel pill will behave differently at operating conditions.

A solution that might help keep the chemicals separated is to increase the viscosity of the gel. However, this will increase the pressure drop over the pill. Using the trend line function of Microsoft Excel an approximation for the viscosity as a function of shear rate is made.

As previously calculated, the shear rate in the system solution is  $160 \text{ s}^{-1}$ . Using the trend line equations, we calculate viscosity which is further used to calculate pressure drops. As before it is assumed a gel pill length of 5 meters between each chemical and 10 meters of each chemical. Over a 30 kilometer long pipe this gives 10000 meters of gel. Table 6.2 shows the pressure drop associated with the different concentrations at the conditions given above. The calculations from Excel are given in figure B.14.

Concentration	Total pressure drop over gel
0.5wt%	490.0 bar
0.75 wt%	779.1 bar
0.1 wt%	1290.5 bar

**Table 6.2:** Pressure drops for different XG gel concentrations over a 30km long pipe.

Even with a concentration of 0.5wt the pressure drop due to friction is quite substantial. And this is only for the separator liquid, or one third of the total pipe length. For the given shear rate, the pressure drops for the higher concentrations are extreme. A rule of thumb often used with regards to pressure supplied by a pump is a maximum of 700 bar. Therefore it is unlikely that higher concentrations are suitable for longer transport. Figure 6.2 shows the pressure drops at different concentration XG gel over different lengths of pipe. The horizontal line is the 700 bar threshold.

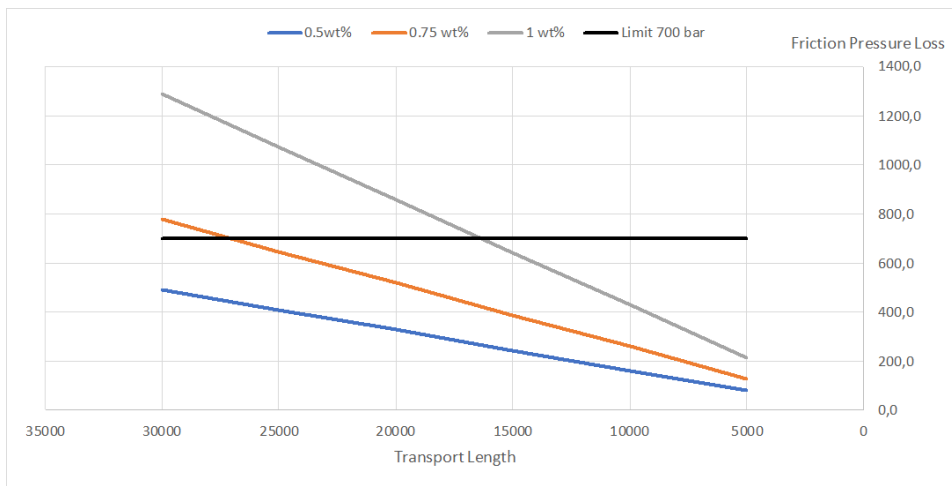


**Figure 6.2:** Pressure drop (bar) of different concentration XG gel at different transport lengths (m).



The flow rate used in the experiment was lower than the one provided by Magnus Lund-Tønnesen from his work on the system side. This was due to the difficulty of balancing the pressures on each side of the loop. The pressure had to be regulated separately for each end due to a minimum operating pressure of the directional valve which far exceeded the pressure needed to push the liquids. If there is an imbalance in the pressures of each end, over time the fluids shift towards one side of the tube. If the fluids are shifted enough to one side there will be overflow. The higher pressures were most unstable, and tended to overflow after a few minutes of operation. This might be due to the pseudoplastic nature of the gel. When the gel flows faster, it exerts less friction. This leads to a situation where small changes in pressure at high flow velocity have a much larger impact than the same change in pressure at low flow velocities. Balancing the lower pressures were easier, and remained more stable over time. However, this did not allow for testing at the flow rates proposed in the system solution.

It seems intuitive that higher flow rates will increase the mixing. With 0.5wt% XG gel, mixing is observed at lower rates than the ones proposed for the system. However, the mixing may be increased due to the back and forth movement in the experimental set-up. Figure 2.8 show the velocity profiles at steady laminar flow. When flow is reversed, the velocity profile will reverse. For the middle of the pipe, the difference will be smaller for the pseudo-plastic fluid than for the other viscosity models. However, closer to the walls the velocity in pseudo-plastic fluids are higher. This may result in more mixing closer to the walls. This can explain why it seemed like the gel seemed to still have about the same viscosity at the end, but looked blue. The glycol is mixed close to the walls, making it appear blue from the outside. But the gel in the middle of the tube is not as mixed and retains its viscosity. A more realistic approach will therefore not have such a high frequency of directional change. A longer tube would allow a further distance to be traveled before changing direction. Therefore, a rig with a longer tube was built.

As the first design of the longer tubed rig did not work as intended. The air used to push the liquids ended up bubbling through the tube rather than pushing the liquids. A second design was proposed and built. The reason the air would bubble through the pipe was assumed to be the lack of pressure on the opposite side, so the liquids settle on the bottom of the tube in some places. This allows air to push through rather than pushing the liquids. In the first design where the tube was hung up in a U, gravity provided a hydrostatic pressure which opposed the pressurized air. The second rig gradually inclined in a coil, as shown in figure 4.7. This way there would always be a difference in height which would act as counter pressure which would keep the liquid filling up the tube rather than settling on the bottom allowing air to bubble through.

When the tube-length was increased to 100 meters, the air pushed the fluids down to the bottom of the vertical section of the tube, then started bubbling through. When pressurized air was applied to the opposite side, the air bubbled through rather than push the liquid back. It was decided that the incline was too small, so there would be some places where the tube sagged between the fastening points. Fastening the tube more tightly would bend the tube too hard and choke the flow. The fluids would gather in the sags, and the air would bubble over. The length was reduced to 50 meters so there was a greater incline. It was still not possible to push the fluids past the bottom of the vertical section without the air bubbling through. It was decided to run the experiment by pushing the liquids only in the

vertical section of the tube. This still represented a significant increase in the travel-length between flow direction changes. However, the gel seemed to break apart and migrate to the ends faster in this configuration. For a run with a gel pill length of 9.7 meters and an  $L$  of 2.3 meters, all observable gel had migrated to the tube ends after 30 minutes. At this time the end of the semester was near, and experiments had to be ended.

It is hard to say whether the increased length of gel pill helped to keep the chemicals separated. The gel seems to break apart and position itself according to density faster when the  $L$  is increased. In a long, flat pipe it is suspected that the gel will not stay as one piece, but break apart and position itself according to density. As mentioned in chapter 2, experiments have been performed where XG gum has been cross-linked. This increased the gel's viscoelastic properties. This may help keep the gel as one piece during use as a spacer liquid.

The problem of air bubbling through rather than pushing the liquids is unrealistic for the system solution. In the real-world application there will be no air in the system. An improvement on experiment 4 in this regard would be to perform the experiment in a closed hydraulic loop. Figure 6.3 shows the improved design for the test loop.

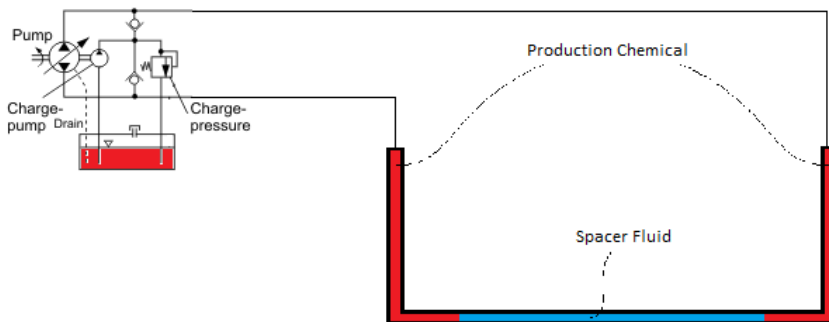


**Figure 6.3:** Loop Design for Improved Experiment

The design shown in figure 6.3 is a closed hydraulic loop. The liquids are propelled by a pump rather than pressurized air, ensuring there is no air in the system. This will make it easier to utilize a larger section of the tube, and not just the vertical parts. It is important to time, or otherwise control the system, to ensure that the spacer fluid does not flow into the tank.

Another possible solution is to build a rig where the liquids are recirculated through the pump. This idea was abandoned for this thesis as it was believed that it would exert too much shear on the liquids, and increase the level of mixing. However, if the change of flow direction is increasing the level of mixing, it is possible that passing the liquids through a low shear pump will result in lower levels of mixing overall. Flanigan et al. (1988) found that a progressive cavity pump exerted the least amount of shear on the liquids it pumped. This is a possible candidate for a pump to use in such a system.

In a progressive cavity pump, the liquid is split into small batches which are pushed

forward. It might be the case that each small batch experience a certain level of mixing due to increased shear from the pump. But the amount of mixing between the batches is small. This may mean that several liquids passing through this pump in succession will not experience increased levels of mixing except in the small batches where two liquids are present. A certain degree of mixing in the interface between the phases is already expected, and it is therefore possible that such a pump will be able to propel the liquids in experiment 4 without too much mixing occurring between the different liquids.

An internal gear pump seems to part the liquid in a similar way as a progressive cavity pump. An internal gear pump may therefore also be a suitable candidate for such a pump. Testing should be done to compare the mixing levels of a few types of pumps to the mixing from frequent directional change.

### **6.4.3 Effect of Residue in Tube**

In total three tubes were used, and the residue was observed in all three. This suggests that it was not a production error, but rather an effect of the use. No residue was observed when the tubes were stored before use, and the amount of residue did not seem to grow when running tests with XG gel and glycol. This suggests that storage conditions are not responsible. The cause is then a condition which occurs during running of water through the hose. It may be the temperature of the water, the water itself or the ambient conditions during testing. The tests were conducted in the same area as the tubes were stored, so it is not likely that the ambient conditions are the cause.

PVC is a polymer, and polymers are known to degrade when exposed to UV-light. Chalking is a phenomenon known to occur in coatings using polymer bindings. This is a degradation of the polymer due to exposure to UV-light. The degradation leaves a white powder. Since the residue did not form during storage, it is possible the addition of water increased the rate of degradation, or the residue is caused by something else.

It might be calcium residue from the water. But, the water in Trondheim is soft, meaning it should not contain much calcium. Calcium residue can also be quite hard to remove, and this residue is removed easily by touch.

The residue did not seem to increase or decrease when tests were run using glycol and XG gel. Two small sections of tube with residue present were cut off. A small sample of glycol and a small sample of 0.5wt% XG gel was put into each of these sections and left overnight. No visible changes were observed in the glycol, gel or tube. It is therefore assumed that the residue is not interfering with the experiments.



# Conclusion and Future Work

## 7.1 Conclusion

Xanthan gum was identified as a possible spacer liquid. Other possible candidates that were identified through the work in this thesis were Scleroglucan and Polyacrylamide. XG was not completely proved effective as a spacer liquids. The viscosity was stable over time and did not change drastically when changing the temperature from around  $20^{\circ}C$  to around  $7^{\circ}C$ . The research seemed to suggest that XG is chemically relatively neutral, and testing did not show any noticeable reaction when exposed to glycol. In dynamic testing, however, XG was not able to keep liquids separate for a longer period of time. But the conditions in testing were not realistic, and more testing should be done in order to finally confirm or dismiss XG as a spacer liquid.

According to the objectives presented in 1.2, the conclusions are as follows:

1. Xanthan gum was identified as a possible spacer liquid and selected for further research. Other possible candidates are Scleroglucan and Polyacrylamide.
2. Xanthan gum:
  - (a) Can keep liquids separated during transport:
    - This was not achieved during this thesis, but further work is needed before a final conclusion is reached.
  - (b) Is compatible with production chemicals:
    - Research suggests XG is chemically very neutral. Testing against glycol showed no adverse effects. Testing against other production chemicals was not achieved.

## **7.2 Future Work**

### **7.2.1 Continue Testing of Xanthan Gum**

More testing of Xanthan gum should be performed. Mainly, a new test rig should be built for experiment 4 where operating conditions are more accurately recreated. This will involve building a rig where the liquids in the tube are propelled by a pump rather than by pressurized air. It should also be looked into whether recirculating the liquids through the pump is a better solution than to push them back and forth. This might lower the levels of mixing due to changes in flow direction and make the test more realistic. To achieve this, low shear pumps should be used so that the liquids experience as little mixing as possible when passing the pump. The author recommends starting with a progressive cavity pump or gear pump. Testing of the pumps effect on the liquid phases should be performed in order to see how passing through the pump compares to flow in a pipe without passing a pump.

Testing of the chemical compatibility between the XG gel and potential chemicals that will be transported with this solution was not achieved in this thesis. The chemicals arrived late, and there was uncertainty surrounding the validity of testing against the chemicals received. This testing needs to be carried out in any future work concerning XG gel as a liquid spacer.

Cross-linked Xanthan gum (CXG) gel have been showed to have an increased viscoelasticity compared to XG gel. Future work should include an evaluation of CXG as a spacer liquid as well. The increased viscoelasticity of the gel may reduce the amount of breakage in the gel. This will in turn reduce the problem of the gel breaking into smaller pieces and migrate through the liquids and settle according to density.

### **7.2.2 Evaluate Other Possible Spacer Liquids**

Two other candidates for spacer liquids were identified in this thesis; Scleroglucan gel and Polyacrylamide gel. Future work should include an evaluation of these possible spacer liquids. Work should be done to identify other possible candidates as well, especially looking into cross-linked polymers. It is believed that cross-linked polymers might be less prone to breaking up into pieces, and thereby be more inclined to keep the liquids separate.

# Bibliography

- Bai, Y. and Bai, Q. (2010a). *Subsea Engineering Handbook*. Elsevier Inc. Chapter 17: Subsea Corrosion and Scale, pages 506–531.
- Bai, Y. and Bai, Q. (2010b). *Subsea Engineering Handbook*. Elsevier Inc. Chapter 17: Subsea Corrosion and Scale, pages 532–539.
- Bai, Y. and Bai, Q. (2010c). *Subsea Engineering Handbook*. Elsevier Inc. Chapter 16: Wax and Asphaltenes, pages 483–504.
- Beaudonnet, G. and Peyrony, V. (2014). Subsea station for chemical storage and injection: 2 case studies. Madrid, Spain. MCE Deepwater Development.
- Bourne, N. (2013). Polymers. In *Materials in Mechanical Extremes*, pages 371–412. Cambridge University Press.
- Buss, F., Roberts, C. C., Crawford, K. S., Peters, K., and Francis, L. F. (2011). Effect of soluble polymer binder on particle distribution in a drying particulate coating. *Journal of Colloid and Interface Science*, 359(1):112–120.
- Carlson, K. A. and Winquist, J. R. (2017). *An Introduction to Statistics: An Active Learning Approach*. SAGE Publications, Inc.
- Darby, R. (2001). Chemical engineering fluid mechanics.
- Dickinson, A., Peck, G. E., and Arnold, B. D. (2005). Effective chemistries to control SRB, h<sub>2</sub>s, and FeS problems. In *SPE Western Regional Meeting*. Society of Petroleum Engineers.
- Ellenberger, J. P. (2014). Piping and pipeline sizing, friction losses, and flow calculations. In *Piping and Pipeline Calculations Manual*, pages 33–54. Elsevier.
- Encyclopædia Britannica (2018). "polymer" in Britannica Academic. URL: <https://academic.eb.com/levels/collegiate/article/polymer/60700>, Accessed 13.03.2018.

- 
- Fann Instrument Company (2016a). Model 140 mud balance instruction manual. Downloaded from: [https://www.fann.com/fann/products/drilling-fluids-testing/mud-balances/mud-balance-m140.html?nodeId=1\\_leveltwo\\_16&pageId=Products&contentType=Procedures%20and%20Manuals&index=0](https://www.fann.com/fann/products/drilling-fluids-testing/mud-balances/mud-balance-m140.html?nodeId=1_leveltwo_16&pageId=Products&contentType=Procedures%20and%20Manuals&index=0), Accessed: 23.05.2018.
- Fann Instrument Company (2016b). Model 35 viscometer instruction manual. Downloaded from: [https://www.fann.com/fann/products/oil-well-cement-testing/viscosity/df-viscosity.html?nodeId=1\\_leveltwo\\_27&contentType=Procedures%20and%20Manuals&index=0](https://www.fann.com/fann/products/oil-well-cement-testing/viscosity/df-viscosity.html?nodeId=1_leveltwo_27&contentType=Procedures%20and%20Manuals&index=0), Accessed: 23.05.2018.
- Fann Instrument Company (2018). Lab equipment product information; mixing/blending/shearing devices. URL: <https://www.fann.com/content/dam/fann/Brochures/Mixers2.pdf>, Accessed: 18.04.2018.
- Fjeldsaunet, K. H. and Lund-Tønnesen, M. (2017). Injection chemical transport system study.
- Flanigan, D., Stolhand, J., Scribner, M., and Shimoda, E. (1988). Droplet size analysis: A new tool for improving oilfield separations. In *SPE Annual Technical Conference and Exhibition*. Society of Petroleum Engineers.
- Hamilton Beach Commercial (2018). Single-spindle drink mixer hmd200 series. Accessed: 18.04.2018; URL = <http://www.hamiltonbeachcommercial.com/en/single-spindle-drink-mixer-hmd200.html>.
- Hand, D. J. (2008). *Statistics: A Very Short Introduction (Very Short Introductions)*. OUP Oxford.
- Heriot-Watt University (2017). URL: [http://www.pet.hw.ac.uk/research/hydrate/hydrates\\_why.cfm](http://www.pet.hw.ac.uk/research/hydrate/hydrates_why.cfm). Accessed: 2017-10-31.
- Holland, F. and Bragg, R. (1995). *Fluid Flow for Chemical and Process Engineers*. Butterworth-Heinemann.
- Hydrauliske Pumper (2000). *Hydraulikk*. NKI Forlaget, Bekkestua.
- Jenkins, A. D., Kratochvíl, P., Stepto, R. F. T., and Suter, U. W. (1996). Glossary of basic terms in polymer science (IUPAC recommendations 1996). *Pure and Applied Chemistry*, 68(12):2287–2311.
- Kang, K. S. and Pettitt, D. J. (1973). *Industrial Gums, Polysaccharides and Their Derivatives, 2nd Edition*. Academic Press Inc.
- Kelland, M. (2014a). *Production chemicals for the oil and gas industry*. Taylor & Francis Group, Boca Raton, Florida, USA, 2nd edition. Chapter 9: Gas Hydrate Control, pages 219–245.
- Kelland, M. (2014b). *Production chemicals for the oil and gas industry*. Taylor & Francis Group, Boca Raton, Florida, USA, 2nd edition. Chapter 3: Scale Control, pages 51–88.



- 
- Kelland, M. (2014c). *Production chemicals for the oil and gas industry*. Taylor & Francis Group, Boca Raton, Florida, USA, 2nd edition. Chapter 4: Asphaltene Control, pages 111–136.
- Kelland, M. (2014d). *Production chemicals for the oil and gas industry*. Taylor & Francis Group, Boca Raton, Florida, USA, 2nd edition. Chapter 11: Demulsifiers, pages 287–301.
- Kelland, M. (2014e). *Production chemicals for the oil and gas industry*. Taylor & Francis Group, Boca Raton, Florida, USA, 2nd edition. Chapter 14: Biocides, pages 327–344.
- Kelland, M. (2014f). *Production chemicals for the oil and gas industry*. Taylor & Francis Group, Boca Raton, Florida, USA, 2nd edition.
- Kokal, S. (2002). Crude oil emulsions: A state-of-the-art review. In *SPE Annual Technical Conference and Exhibition*. Society of Petroleum Engineers.
- Lundal, V. and Festøy, S. v. D. (2017). A study of a subsea chemicals storage & injection-station.
- Mackay, E. (2008). Oilfield scale: A new integrated approach to tackle an old foe. SPE-120503-DL.
- Merriam-Webster Online Dictionary (2018). Viscosity. <https://www.merriam-webster.com/dictionary/viscosity>, Accessed: 30.04.2018.
- Microsoft (2018). *Correl function*. support.office.com. URL: <https://support.office.com/en-us/article/correl-function-995dcef7-0c0a-4bed-a3fb-239d7b68ca92>, Accessed: 18.05.2018.
- Nesbitt, B. (2007). Valves manual international : handbook of valves and acutators.
- Patrick, S. S. (2005). *Practical guide to polyvinyl chloride*. Rapra Technology, Shrewsbury, Shropshire, UK.
- Rennels, D. C. and Hudson, H. M. (2012). Valves. In *Pipe Flow*, pages 205–212. John Wiley & Sons, Inc.
- rheosense.com (2018). Viscosity of newtonian and non-newtonian fluids. URL: <http://www.rheosense.com/applications/viscosity/newtonian-non-newtonian>, Accessed: 19.05.2018.
- Santos, D., Brites, C., Costa, M., and Santos, M. (2005). Performance of paint systems with polyurethane topcoats, proposed for atmospheres with very high corrosivity category. *Progress in Organic Coatings*, 54(4):344–352.
- Sartorius (2017). User manual: Secura, quintix, practicum laboratory balances. Downloaded from: [https://www.sartorius.com/sartorius/en/EUR/Applications/Laboratory/Weighing/Laboratory-Balances/Quintix%C2%AE/p/M\\_Quintix\\_Laboratory\\_Balances](https://www.sartorius.com/sartorius/en/EUR/Applications/Laboratory/Weighing/Laboratory-Balances/Quintix%C2%AE/p/M_Quintix_Laboratory_Balances), Accessed: 23.05.2018.
-

- 
- Schlumberger Oilfield Glossary (2017). Xanthan gum. URL: [http://www.glossary.oilfield.slb.com/en/Terms/x/xanthan\\_gum.aspx](http://www.glossary.oilfield.slb.com/en/Terms/x/xanthan_gum.aspx), Accessed: 18.05.2018.
- Schroeder, L., Sjoquist, D., and Stephan, P. (1986). *Understanding Regression Analysis*. SAGE Publications, Inc.
- Schwerdtfeger, T., van den Akker, J., Scott, B., and Chakkungal, J. (2017). World first all electric subsea well. In *SPE Offshore Europe Conference & Exhibition*. Society of Petroleum Engineers.
- Skovhus, T. L., Enning, D., and Lee, J. S. (2017). Microbiologically influenced corrosion in the upstream oil and gas industry. p. 15.
- SkySpring, Oil and Gas Service, Inc (2017). URL: <http://ssoag.com/products-services/asphaltene-solvent-ss220-and-ss622/>. Accessed: 2017-10-31.
- Sumathi, S. (2007). *LabVIEW based Advanced Instrumentation Systems*. Springer Berlin Heidelberg, Berlin/Heidelberg.
- Sworn, G. (2009). Xanthan gum. In *Handbook of Hydrocolloids*, pages 186–203. Elsevier.
- The University of Kansas (2017). URL: <https://torp.ku.edu/wax-deposition>. Accessed: 2017-10-31.
- Turkiewicz, A., Brzeszcz, J., and Kapusta, P. (2013). The application of biocides in the oil and gas industry. Oil and Gas Institute, Krakow.
- Wahren, U. (1997). *Practical Introduction to Pumping Technology*. Elsevier.
- Wen, J., Zhao, K., Gu, T., and Nestic, S. (2006). Effects of mass transfer and flow conditions on srb corrosion of mild steel. San Diego, California, USA. NACE International: CORROSION.
- Wikipedia (2018a). URL: [https://en.wikipedia.org/wiki/Couette\\_flow](https://en.wikipedia.org/wiki/Couette_flow), Accessed: 15.05.2018.
- Wikipedia (2018b). URL: [https://en.wikipedia.org/wiki/Gear\\_pump](https://en.wikipedia.org/wiki/Gear_pump), Accessed: 27.05.2018.
- Wikipedia (2018c). URL: [https://en.wikipedia.org/wiki/Lobe\\_pump](https://en.wikipedia.org/wiki/Lobe_pump), Accessed: 27.05.2018.
- Zhang, H., Fang, B., Lu, Y., Qiu, X., Jin, H., Liu, Y., Wang, L., Tian, M., and Li, K. (2016). Rheological properties of water-soluble cross-linked xanthan gum. *Journal of Dispersion Science and Technology*, 38(3):361–366.

# Appendices



# Appendix A

## Tables

Speed (RPM)	Shear Rate ( $s^{-1}$ )
3	5.11
6	10.21
100	170.23
200	340.46
300	510.69
600	1021.38

**Table A.1:** RPM and corresponding shear rate in  $s^{-1}$  for the Fann viscometer.

Rotor - Bob Combination	R-B Factor (C)
R1 B1	1.000
R1 B2	8.915
R1 B3	25.329
R1 B4	50.787
R2 B1	0.315
R2 B2	8.229
R2 B3	24.707
R2 B4	49.412
R3 B1	4.517
R3 B2	12.431
R3 B3	28.909
R3 B4	57.815

**Table A.2:** Rotor - Bob Factors for the Fann viscometer.

Speed (RPM)	Speed Factor (S)
3	100
6	50
100	3
200	1.5
300	1
600	0.5

**Table A.3:** Speed factors for the Fann viscometer.

<i>df</i>	$\alpha = .05$	$\alpha = .01$	<i>df</i>	$\alpha = .05$	$\alpha = .01$	<i>df</i>	$\alpha = .05$	$\alpha = .01$	<i>df</i>	$\alpha = .05$	$\alpha = .01$
1	0.988	1.000	31	0.291	0.403	61	0.209	0.293	91	0.172	0.241
2	0.900	0.980	32	0.287	0.397	62	0.207	0.290	92	0.171	0.240
3	0.805	0.934	33	0.283	0.392	63	0.206	0.288	93	0.170	0.238
4	0.729	0.882	34	0.279	0.386	64	0.204	0.286	94	0.169	0.237
5	0.669	0.833	35	0.275	0.381	65	0.203	0.284	95	0.168	0.236
6	0.621	0.789	36	0.271	0.376	66	0.201	0.282	96	0.167	0.235
7	0.582	0.750	37	0.267	0.371	67	0.200	0.280	97	0.166	0.234
8	0.549	0.715	38	0.264	0.367	68	0.198	0.278	98	0.165	0.232
9	0.521	0.685	39	0.260	0.362	69	0.197	0.276	99	0.165	0.231
10	0.497	0.658	40	0.257	0.358	70	0.195	0.274	100	0.164	0.230
11	0.476	0.634	41	0.254	0.354	71	0.194	0.272	101	0.163	0.229
12	0.458	0.612	42	0.251	0.350	72	0.193	0.270	102	0.162	0.228
13	0.441	0.592	43	0.248	0.346	73	0.191	0.268	103	0.161	0.227
14	0.426	0.574	44	0.246	0.342	74	0.190	0.266	104	0.161	0.226
15	0.412	0.558	45	0.243	0.338	75	0.189	0.265	105	0.160	0.225
16	0.400	0.543	46	0.240	0.335	76	0.188	0.263	106	0.159	0.224
17	0.389	0.529	47	0.238	0.331	77	0.186	0.261	107	0.158	0.223
18	0.378	0.516	48	0.235	0.328	78	0.185	0.260	108	0.158	0.222
19	0.369	0.503	49	0.233	0.325	79	0.184	0.258	109	0.157	0.221
20	0.360	0.492	50	0.231	0.322	80	0.183	0.257	110	0.156	0.220
21	0.352	0.482	51	0.228	0.319	81	0.182	0.255	111	0.156	0.219
22	0.344	0.472	52	0.226	0.316	82	0.181	0.253	112	0.155	0.218
23	0.337	0.462	53	0.224	0.313	83	0.180	0.252	113	0.154	0.217
24	0.330	0.453	54	0.222	0.310	84	0.179	0.251	114	0.153	0.216
25	0.323	0.445	55	0.220	0.307	85	0.178	0.249	115	0.153	0.215
26	0.317	0.437	56	0.218	0.305	86	0.176	0.248	116	0.152	0.214
27	0.311	0.430	57	0.216	0.302	87	0.175	0.246	117	0.152	0.213
28	0.306	0.423	58	0.214	0.300	88	0.174	0.245	118	0.151	0.212
29	0.301	0.416	59	0.213	0.297	89	0.174	0.244	119	0.150	0.211
30	0.296	0.409	60	0.211	0.295	90	0.173	0.242	120	0.150	0.210

**Figure A.1:** Pearson Correlation Table (Carlson and Winquist, 2017).

# Appendix **B**

## Results from Experiments

### B.1 Experiment 1

#### B.1.1 Viscosity Measurements

Date	Shear Rate						Temperature
	5.1	170.2	510.7	10.2	340.5	1021.4	
06.02	4100	243	105	2400	142.5	63.5	22.2 °C
09.02	4100	252	106	2350	144	65.5	20.7 °C
12.02	5700	270	116	3150	174	72	20.2 °C
14.02	6900	285	122	3600	165	73.5	21.4 °C
16.02	5800	285	122	3600	165	74.5	20.7 °C
19.02	5700	276	122	3500	168	75	21 °C
21.02	5900	279	123	3550	166.5	74.5	21.3 °C
23.02	6700	279	123	3550	166.5	74.5	19.9 °C
26.02	6600	285	122	3500	165	74	19.3 °C
28.02	6300	273	120	3500	177	70.5	20.8 °C
02.03	6200	261	119	3400	175.5	70.5	22.3 °C
07.03	6200	264	115	3300	171	68.5	22.3 °C
14.03	6100	258	111	3150	151.5	66.5	20.4 °C

**Table B.1:** Viscosity measurements 1.5wt% XG solution, room temperature storage

---

Date	Shear Rate						Temperature
	5.1	170.2	510.7	10.2	340.5	1021.4	
06.02	4100	246	109	2400	145.5	67.5	20.8 °C
09.02	4200	255	115	2250	147	70.5	6.9 °C
12.02	4000	243	112	2400	163.5	71	5.7 °C
14.02	4100	249	112	2350	150	70.5	6.9 °C
16.02	3900	243	111	2250	150	71.5	6.2 °C
19.02	4000	252	112	2300	151.5	71	6.1 °C
21.02	4100	255	115	2400	169.5	72.5	6.2 °C
23.02	4000	252	114	2350	153	72	5.5 °C
26.02	4200	258	111	2450	156	73	7.2 °C
28.02	4200	258	117	2450	157.5	74	5.9 °C
02.03	4700	267	120	2500	174	74.5	6.6 °C
07.03	4300	258	120	2750	162	76	6.2 °C
14.03	5100	273	124	2900	166.5	78	6.1 °C

**Table B.2:** Viscosity measurements 1.5wt% XG solution, cold storage

Date	Shear Rate						Temperature
	5.1	170.2	510.7	10.2	340.5	1021.4	
06.02	2800	141	64	1450	84	40	20.7 °C
09.02	3000	153	68	1600	91.5	41	20.5 °C
12.02	3700	177	78	2050	103.5	47	20.1 °C
14.02	3500	174	77	1950	103.5	46.5	21.5 °C
16.02	3700	177	78	1950	103.5	47	20 °C
19.02	3700	177	78	1950	105	47	19.7 °C
21.02	3700	174	75	1900	100.5	45.5	20.3 °C
23.02	3500	171	75	1850	93	45	19.8 °C
26.02	3300	168	74	1800	99	44.5	19.3 °C
28.02	3100	162	71	1750	96	43	20.6 °C
02.03	3000	162	71	1700	96	42	22.4 °C
07.03	3000	156	68	1600	91.5	40	22.3 °C
14.03	1400	96	44	850	58.5	27	20.3 °C

**Table B.3:** Viscosity measurements 1wt% XG solution, room temperature storage

---



---

Date	Shear Rate						Temperature
	5.1	170.2	510.7	10.2	340.5	1021.4	
06.02	3000	147	69	1600	91.5	42	20.4 °C
09.02	2800	159	76	1600	100.5	47	5.9 °C
12.02	2800	162	73	1600	99	47	6.3 °C
14.02	2900	156	74	1600	99	47	5.9 °C
16.02	2900	159	74	1600	99	47	5.8 °C
19.02	2900	159	73	1600	99	47	6.2 °C
21.02	2900	165	74	1600	99	46.5	5.9 °C
23.02	2900	162	74	1600	99	47	5.4 °C
26.02	2800	165	74	1650	100.5	47.5	5.7 °C
28.02	2700	162	75	1650	100.5	47	7.1 °C
02.03	2900	165	74	1650	99	47.5	7.3 °C
07.03	3100	168	72	1750	102	48	6.2 °C
14.03	3000	162	75	1750	103.5	48	7.4 °C

**Table B.4:** Viscosity measurements 1wt% XG solution, cold storage

Date	Shear Rate						Temperature
	5.1	170.2	510.7	10.2	340.5	1021.4	
06.02	700	48	24	400	31.5	18	19.2 °C
09.02	1400	66	32	750	42	19.5	20.5 °C
12.02	1000	69	32	650	42	20	20.2 °C
14.02	900	63	30	500	39	19	21 °C
16.02	900	63	30	500	39	18.5	21.3 °C
19.02	800	63	29	550	37.5	15.5	20.6 °C
21.02	800	60	28	500	37.5	17.5	19.3 °C
23.02	800	60	28	450	36	17.5	19.8 °C
26.02	800	57	27	450	36	17	19.2 °C
28.02	700	57	26	450	34.5	16.5	20.8 °C
02.03	700	54	26	450	34.5	16	22.5 °C
07.03	700	51	24	450	31.5	15.5	22.3 °C
14.03	-	-	-	-	-	-	- °C

**Table B.5:** Viscosity measurements 0.5wt% XG solution, room temperature storage

Date	Shear Rate						Temperature
	5.1	170.2	510.7	10.2	340.5	1021.4	
06.02	1200	63	30	650	39	19	21.3 °C
09.02	1300	66	32	650	42	20.5	6.1 °C
12.02	1200	63	31	650	40.5	20.5	5.9 °C
14.02	1200	63	32	650	42	20.5	6.5 °C
16.02	1200	63	32	650	42	20	5.7 °C
19.02	1200	63	31	650	40.5	20	6.3 °C
21.02	1300	63	31	650	40.5	20	6.2 °C
23.02	1200	63	31	650	40.5	20	6.9 °C
26.02	1200	66	32	650	42	20.5	5.8 °C
28.02	1100	66	32	650	42	20.5	6.1 °C
02.03	1200	63	31	650	40.5	20.5	6.2 °C
07.03	1100	63	31	650	40.5	20	7.2 °C
14.03	1200	66	31	650	42	20	5.9 °C

**Table B.6:** Viscosity measurements 0.5wt% XG solution, cold storage

### Correlation Calculations

The correlation coefficients in this are calculated using the *Correlation* data analysis tool in Excel. The output is a table with the different variables. The correlation coefficient of variables are given in the intersection between the two variables. The variables are named Viscosity;RPM<sub>i</sub>, so for instance the variable *Viscosity3* is the viscosity measured at 3 RPM in the Fann viscometer. For a conversion between RPM and shear rate in reciprocal seconds, consult table A.1.

	Viscosity3	Viscosity100	Viscosity300	Viscosity6	Viscosity200	Viscosity600	Temperature	Days	Average
Viscosity3	1								
Viscosity100	0,74621473	1							
Viscosity300	0,80418079	0,9263316	1						
Viscosity6	0,89886311	0,87522948	0,95590131	1					
Viscosity200	0,71792257	0,60493281	0,76606129	0,79176309	1				
Viscosity600	0,67478051	0,94066322	0,95729549	0,86672266	0,66937221	1			
Temperature	-0,2614508	-0,4711378	-0,27952899	-0,21404477	-0,01979599	-0,39535891	1		-0,27355288
Days	0,58103972	0,07403197	0,21155764	0,43075621	0,35031875	0,02241951	-0,02558384	1	0,27835397

**Figure B.1:** Correlation table for measurements on the 1.5wt% sample at room storage.

	Viscosity3	Viscosity100	Viscosity300	Viscosity6	Viscosity200	Viscosity600	Temperature	Days	Average
Viscosity3	1								
Viscosity100	0,90745968	1							
Viscosity300	0,84677513	0,86605137	1						
Viscosity6	0,81008819	0,72845361	0,79689536	1					
Viscosity200	0,58064872	0,60315235	0,67543684	0,5699846	1				
Viscosity600	0,74929861	0,81969145	0,89616255	0,82305049	0,69347979	1			
Temperature	-0,09496768	-0,27035764	-0,40860837	-0,08027677	-0,41212767	-0,55992841	1		-0,30437776
Days	0,72638744	0,83066139	0,8379306	0,82692641	0,65037926	0,96803452	-0,45932949	1	0,80671994

**Figure B.2:** Correlation table for measurements on the 1.5wt% sample at cold storage.

	Viscosity3	Viscosity100	Viscosity300	Viscosity6	Viscosity200	Viscosity600	Temperature	Days	Average
Viscosity3	1								
Viscosity100	0,98525919	1							
Viscosity300	0,98581796	0,99721244	1						
Viscosity6	0,98404559	0,99203199	0,99318377	1					
Viscosity200	0,9623949	0,9832352	0,98419578	0,97888346	1				
Viscosity600	0,98814471	0,98762219	0,99476333	0,98936908	0,97642803	1			
Temperature	-0,2002305	-0,11697983	-0,13618368	-0,15552912	-0,07151307	-0,18499716	1		-0,14423889
Days	-0,55244889	-0,46754102	-0,51542315	-0,50588784	-0,49373275	-0,5775012	0,23773846	1	-0,51875581

**Figure B.3:** Correlation table for measurements on the 1wt% sample at room storage.

	Viscosity3	Viscosity100	Viscosity300	Viscosity6	Viscosity200	Viscosity600	Temperature	Days	Average
Viscosity3	1								
Viscosity100	-0,06325492	1							
Viscosity300	-0,53471781	0,5012587	1						
Viscosity6	0,484411	0,4897925	0,06421265	1					
Viscosity200	-0,07751889	0,78000413	0,74874342	0,61162534	1				
Viscosity600	-0,14341854	0,83461744	0,74491426	0,43504795	0,93736256	1			
Temperature	0,31224974	-0,75987553	-0,78369241	-0,09862161	-0,80970411	-0,92522938	1		-0,51081222
Days	0,28044363	0,69218601	0,30253889	0,86304692	0,71190499	0,62501117	-0,35630221	1	0,5791886

**Figure B.4:** Correlation table for measurements on the 1wt% sample at cold storage.

	Viscosity3	Viscosity100	Viscosity300	Viscosity6	Viscosity200	Viscosity600	Temperature	Days	Average
Viscosity3	1								
Viscosity100	0,70635083	1							
Viscosity300	0,80835119	0,97429047	1						
Viscosity6	0,92310423	0,78994611	0,83558004	1					
Viscosity200	0,81399853	0,96673959	0,99201025	0,84716388	1				
Viscosity600	0,7058904	0,603791	0,71453743	0,58498968	0,71925937	1			
Temperature	-0,10135273	-0,10071847	-0,11383617	-0,01710477	-0,1359685	-0,34182094	1		-0,1351336
Days	-0,57166156	-0,40031338	-0,5357227	-0,48171821	-0,51453018	-0,78317975	0,48459802	1	-0,5478543

**Figure B.5:** Correlation table for measurements on the 0.5wt% sample at room storage.

	Viscosity3	Viscosity100	Viscosity300	Viscosity6	Viscosity200	Viscosity600	Temperature	Days	Average
Viscosity3	1								
Viscosity100	0	1							
Viscosity300	0	0,48683382	1						
Viscosity6	#DIV/0!	#DIV/0!	#DIV/0!	1					
Viscosity200	0	0,65648795	0,90669283	#DIV/0!	1				
Viscosity600	0	0,35902456	0,73746841	#DIV/0!	0,66865732	1			
Temperature	-0,03438884	-0,23558237	-0,6487697	#DIV/0!	-0,67458937	-0,82683101	1		-0,48403226
Days	-0,45430643	0,30673198	0,00678884	#DIV/0!	0,25567614	0,19096426	-0,42816682	1	0,06117096

**Figure B.6:** Correlation table for measurements on the 0.5wt% sample at cold storage.

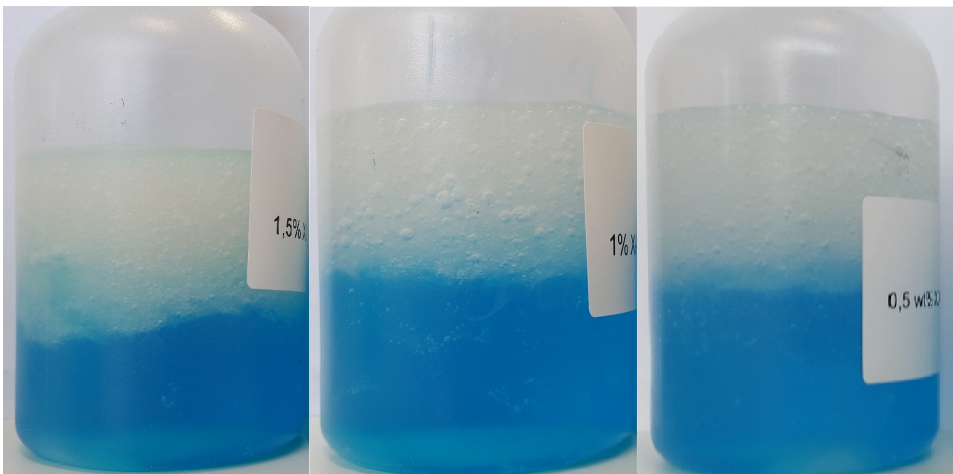
## B.1.2 Density Measurements

Table B.7 shows the density measurements of the six samples in  $g/cm^3$ . RT stands for room temperature, and CS stands for cold storage.

Date	1.5wt% RT	1.5wt% CS	1wt% RT	1wt% CS	0.5wt% RT	0.5wt% CS
06.02	0.96	0.97	0.97	0.97	0.98	0.98
09.02	0.96	0.97	0.98	0.97	0.98	0.98
16.02	0.97	0.96	0.98	0.98	1	0.98
23.02	0.97	0.97	0.98	0.98	1	0.98
02.03	1	0.98	1	0.98	1	1
14.03	1	0.99	1	0.99	-	1

**Table B.7:** Density measurements for experiment 1

## B.2 Experiment 2



**Figure B.7:** All bottles on day of mix.

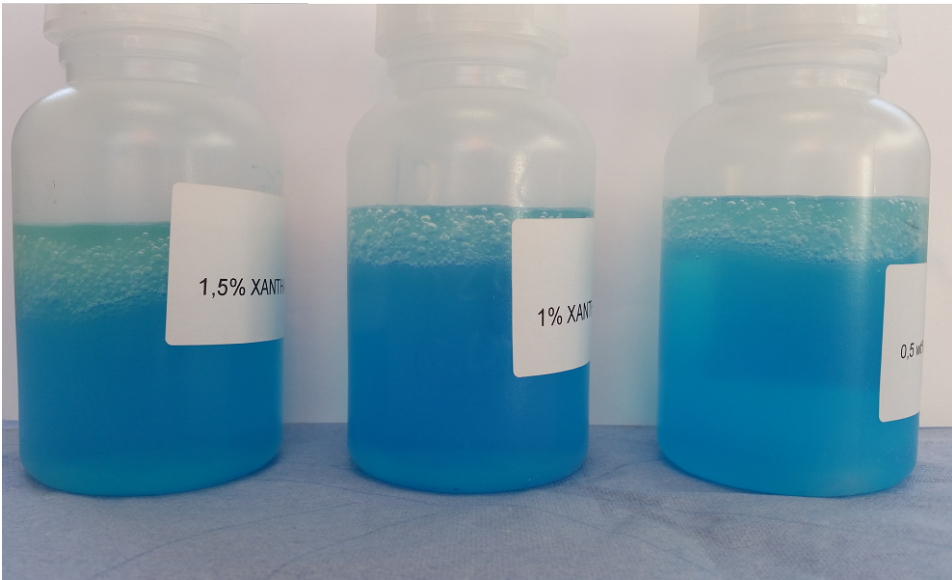


**Figure B.8:** All bottles 7 days after mix.

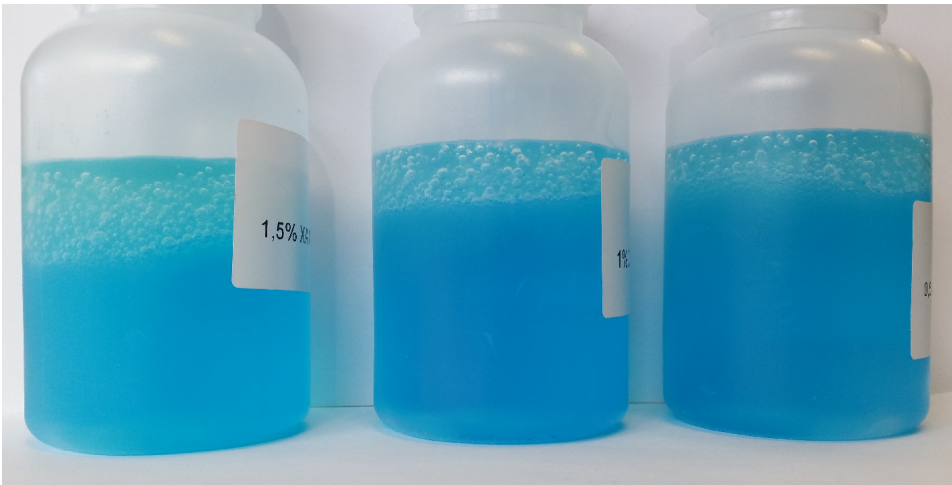


**Figure B.9:** All bottles 30 days after mix.

### B.3 Experiment 3

Date	$5.1s^{-1}$		$170.2s^{-1}$		$510.7s^{-1}$		$10.2s^{-1}$		$340.5s^{-1}$		$1021.4s^{-1}$	
	cP	$^{\circ}C$	cP	$^{\circ}C$	cP	$^{\circ}C$	cP	$^{\circ}C$	cP	$^{\circ}C$	cP	$^{\circ}C$
06.04	1200	27.1	60	27.2	28	27.2	650	27.0	36	26.8	17	26.7
13.04	1300	7.9	69	8.0	33	8.3	700	8.7	43.5	9.7	21.5	10.3
20.04	1400	6.7	72	6.7	34	6.8	750	7.0	45	7.3	21.5	7.4
27.04	1300	7.2	69	7.3	33	7.3	700	7.8	43.5	7.8	21	8.9
03.05	1300	7.9	66	7.2	32	7.2	700	7.5	42	7.5	20.5	7.9
11.05	1200	6.9	63	7.0	31	7.0	700	7.4	42	7.5	20	8.4
18.05	1300	6.0	66	6.0	32	6.2	700	6.8	43.5	6.8	20.5	8.1
25.05	1300	7.0	66	7.0	32	7.1	700	7.5	42	7.8	20.5	8.5

**Table B.8:** Viscosity measurements 0.5wt% XG solution, cold storage

Figure B.10 shows the viscosity measurements from experiment 1 on top, and results from experiment 3 on the bottom. The second to last row contains the p-values from a t-test on the data sets above.

Experiment 1												
Date	3 RPM		100 RPM		300 RPM		6 RPM		200 RPM		600 RPM	
	Speedfactor	Viscosity	Speedfactor	Viscosity	Speedfactor	Viscosity	Speedfactor	Viscosity	Speedfactor	Viscosity	Speedfactor	Viscosity
06.feb	12	1200	21	63	30	30	13	650	26	39	38	19
09.feb	13	1300	22	66	32	32	13	650	28	42	41	20.5
12.feb	12	1200	21	63	31	31	13	650	27	40.5	41	20.5
14.feb	12	1200	21	63	32	32	13	650	28	42	41	20.5
16.feb	12	1200	21	63	32	32	13	650	28	42	40	20
19.feb	12	1200	21	63	31	31	13	650	27	40.5	40	20
21.feb	13	1300	21	63	31	31	13	650	27	40.5	40	20
23.feb	12	1200	21	63	31	31	13	650	27	40.5	40	20
26.feb	12	1200	22	66	32	32	13	650	28	42	41	20.5
28.feb	11	1100	22	66	32	32	13	650	28	42	41	20.5
02.mar	12	1200	21	63	31	31	13	650	27	40.5	41	20.5
07.mar	11	1100	21	63	31	31	13	650	27	40.5	40	20
14.mar	12	1200	22	66	31	31	13	650	28	42	40	20
Experiment 3												
06.apr	12	1200	20	60	28	28	13	650	24	36	34	17
13.apr	13	1300	23	69	33	33	14	700	29	43.5	43	21.5
20.apr	14	1400	24	72	34	34	15	750	30	45	43	21.5
27.apr	13	1300	23	69	33	33	14	700	29	43.5	42	21
03.mai	13	1300	22	66	32	32	14	700	28	42	41	20.5
11.mai	12	1200	21	63	31	31	14	700	28	42	40	20
18.mai	13	1300	22	66	32	32	14	700	29	43.5	41	20.5
25.mai	13	1300	22	66	32	32	14	700	28	42	41	20.5
T-test (p-value)	0,00433767		0,04497394		0,30839559		1,52058E-06		0,19024065		0,71032479	
Different Mean	Yes		Yes		No		Yes		No		No	

**Figure B.10:** Comparison of results from experiment 1 and 3.

	Shear Rate ( $s^{-1}$ )						
	5.1	170.2	510.7	10.2	340.5	1021.4	
Adjusted $R^2$	0.22	0.67	0.85	0.58	0.90	0.90	
$R^2$ Temp	0.31	0.46	0.73	0.60	0.84	0.82	
$R^2$ Time	0.002	0.0005	0.04	0.05	0.12	0.09	

**Table B.9:** Squared correlation coefficients for results from experiment 3.

	5,11 s <sup>-1</sup>	Temp	Time		170,23 s <sup>-1</sup>	Temp	Time		510,69 s <sup>-1</sup>	Temp	Time
5,11 s <sup>-1</sup>	1,00			170,23 s <sup>-1</sup>	1,00			510,69 s <sup>-1</sup>	1,00		
Temp	-0,81	1,00		Temp	-0,89	1,00		Temp	-0,96	1,00	
Time	0,46	-0,74	1,00	Time	0,44	-0,73	1,00	Time	0,55	-0,74	1,00
	10,21 s <sup>-1</sup>	Temp	Time		340,46 s <sup>-1</sup>	Temp	Time		1021,38 s <sup>-1</sup>	Temp	Time
10,21 s <sup>-1</sup>	1,00			340,46 s <sup>-1</sup>	1,00			1021,38 s <sup>-1</sup>	1,00		
Temp	-0,82	1,00		Temp	-0,95	1,00		Temp	-0,96	1,00	
Time	0,46	-0,74	1,00	Time	0,55	-0,77	1,00	Time	0,56	-0,77	1,00

**Figure B.11:** Correlation table for measurements in experiment3.

Date	Density (g/cm <sup>3</sup> )
06.04	0.98
13.04	0.98
20.04	0.97
27.04	0.99
03.05	0.99
11.05	1.00
18.05	1.00
25.05	1.00

**Table B.10:** Density measurements from experiment 3.

---

## B.4 Experiment 4

### B.4.1 Initial Runs

Date	10.apr	Date	13.apr
Gel lenght Measured Start	3,50 m	Gel lenght Measured Start	3,40 m
Gel lenght Measured End	2,80 m	Gel lenght Measured End	0,00 m
Time Position 1	10,00 s	Time Position 1	8,00 s
Time Position 2	11,00 s	Time Position 2	10,00 s
L Position 1 to Position 2	0,38 m	L Position 1 to Position 2	0,42 m
Total Run Time	2,00 hr	Total Run Time	4,00 hr
Flow Velocity	0,04 m/s	Flow Velocity	0,05 m/s
Total Simulated Length	260,57 m	Total Simulated Length	672,00 m
Percent Reduction	20 %	Percent Reduction	100 %
Date	17.apr	Date	24.apr
Gel lenght Measured Start	4,60 m	Gel lenght Measured Start	4,90 m
Gel lenght Measured End	0,00 m	Gel lenght Measured End	0,00 m
Time Position 1	10,00 s	Time Position 1	8,00 s
Time Position 2	9,00 s	Time Position 2	9,00 s
L Position 1 to Position 2	0,18 m	L Position 1 to Position 2	0,21 m
Total Run Time	5,00 hr	Total Run Time	5,00 hr
Flow Velocity	0,02 m/s	Flow Velocity	0,02 m/s
Total Simulated Length	341,05 m	Total Simulated Length	444,71 m
Percent Reduction	100 %	Percent Reduction	100 %

**Figure B.12:** Results from initial runs of experiment 4.



## B.4.2 Higher Concentration Runs

0.75wt% XG gel			
Date	08.mai	Date	09.mai
Gel lenght Measured Start	4,80 m	Gel lenght Measured Start	4,90 m
Gel lenght Measured End	2,80 m	Gel lenght Measured End	0,00 m
Time Position 1	16,00 s	Time Position 1	17,00 s
Time Position 2	13,00 s	Time Position 2	15,00 s
L Position 1 to Position 2	0,26 m	L Position 1 to Position 2	0,24 m
Total Run Time	5,00 hr	Total Run Time	5,00 hr
Flow Velocity	0,02 m/s	Flow Velocity	0,02 m/s
Total Simulated Length	322,76 m	Total Simulated Length	270,00 m
Percent Reduction	42 %	Percent Reduction	100 %
1wt% XG gel			
Date	14.mai	Date	16.mai
Gel lenght Measured Start	4,70 m	Gel lenght Measured Start	4,90 m
Gel lenght Measured End	0,00 m	Gel lenght Measured End	0,00 m
Time Position 1	18,00 s	Time Position 1	14,00 s
Time Position 2	15,00 s	Time Position 2	15,00 s
L Position 1 to Position 2	0,26 m	L Position 1 to Position 2	0,21 m
Total Run Time	4,50 hr	Total Run Time	5,00 hr
Flow Velocity	0,02 m/s	Flow Velocity	0,01 m/s
Total Simulated Length	255,27 m	Total Simulated Length	260,69 m
Percent Reduction	100 %	Percent Reduction	100 %

**Figure B.13:** Results from runs of experiment 4 with higher concentration XG gels.

Transport length	30000 m		Trend Line Equations		
			0,5wt%	0,75wt%	1wt%
Chemtrain length	75 m				
N chemtrains	400	$ax^b$	$4031,2x^{(-0,781)}$	$7655,4x^{(-0,816)}$	$13684x^{(-0,831)}$
Total gel length	10000 m	a	4031	7655,4	13684
Diameter	0,01 m	b	-0,781	-0,816	-0,831
Flow Velocity	0,2 m/s				
Density	980 kg/m <sup>3</sup>				
Shear Rate	160 s <sup>-1</sup>	$*(8*B6)/B5$			
Viscosity 0,5wt%	76,6 cP	$*=E4*B9^{(E5)}$			
Viscosity 0,75wt%	121,7 cP	$*=F4*B9^{(F5)}$			
Viscosity 1wt%	201,6 cP	$*=G4*B9^{(G5)}$			
Reynolds 0,5wt%	25,6	$*(B\$8*B\$6*0,01)/(B11/1000)$			
Reynolds 0,75wt%	16,1	$*(B\$8*B\$6*0,01)/(B12/1000)$			
Reynolds 1wt%	9,7	$*(B\$8*B\$6*0,01)/(B13/1000)$			
Friction factor 0,5wt%	2,5	$*=64/B15$			
Friction factor 0,75wt%	4,0	$*=64/B16$			
Friction factor 1wt%	6,6	$*=64/B17$			
Pressure loss 0,5wt%	490,0 Bar	$*(B19*(980/2)*((0,2^2)/0,01)*B\$4)/(10^5)$			
Pressure loss 0,75wt%	779,1 Bar	$*(B20*(980/2)*((0,2^2)/0,01)*B\$4)/(10^5)$			
Pressure loss 1wt%	1290,5 Bar	$*(B21*(980/2)*((0,2^2)/0,01)*B\$4)/(10^5)$			

**Figure B.14:** Pressure drop calculations for different viscosities

# Appendix C

## LabVIEW Programming

As discussed in section 3.4.5, LabVIEW was used for automating the alternating pressure application in experiment 4. This section will give an overview of the programming solution. Figure C.1 shows the block diagram of the valve automation VI.

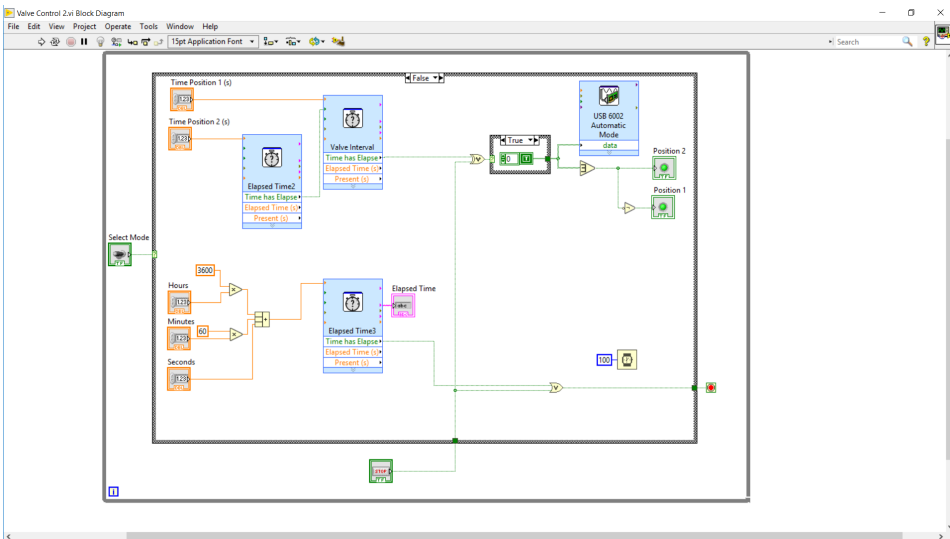
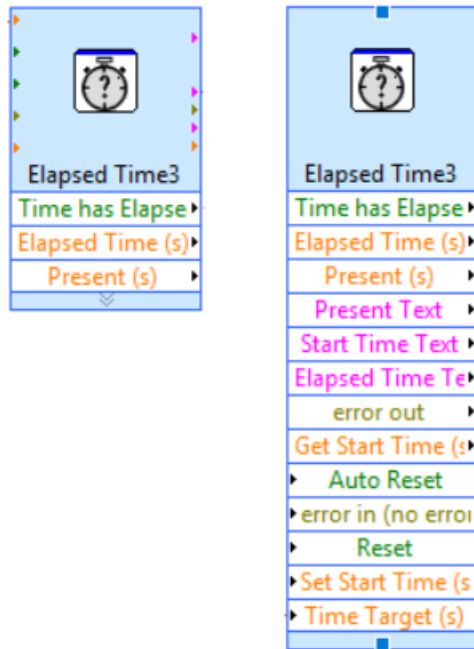


Figure C.1: Block diagram for the valve control automation.

It proved more difficult than anticipated to program the automatic alternation of the valve. It was assumed that there was a sub-VI available that would deliver an alternating on-off signal. This was not the case, and it was necessary to build this from the ground up.

This was achieved using the *Elapsed Time* sub-VI. A sub-VI is a VI which is used inside another VI. Figure C.2 shows the *Elapsed Time* sub-VI.



**Figure C.2:** Left: Collapsed *Elapsed Time* sub-VI. Right: Expanded *Elapsed Time* sub-VI.

The left side shows the *Elapsed Time* sub-VI as it is shown in C.1. The right side of figure C.2 shows the same VI in its expanded state. The colored triangles on the sub-VI shown on the left side corresponds with the colored names in the sub-VI on the right. The side on which the black triangle is on in the elapsed state, is the same side as the corresponding colored triangle is on in the collapsed state. These are different ports for the sub-VI. Triangles on the left indicate input ports, triangles on the right are output ports. The ports used in the block diagram for the valve control are:

- Time has Elapsed (output)
- Elapsed Time Text (output)
- Reset (input)
- Time Target (s) (input)

*Time has Elapsed* outputs a boolean signal. When elapsed time is less than the time target, this is false, When the time target is reached, this is true. *Elapsed Time Text* outputs elapsed time as a text-string with the format hh:mm:ss. Reset accepts a boolean signal as an input, and when the input is true the elapsed time is reset to 0. *Time Target (s)* accepts an integer as input, and this number is set as the target time in seconds.

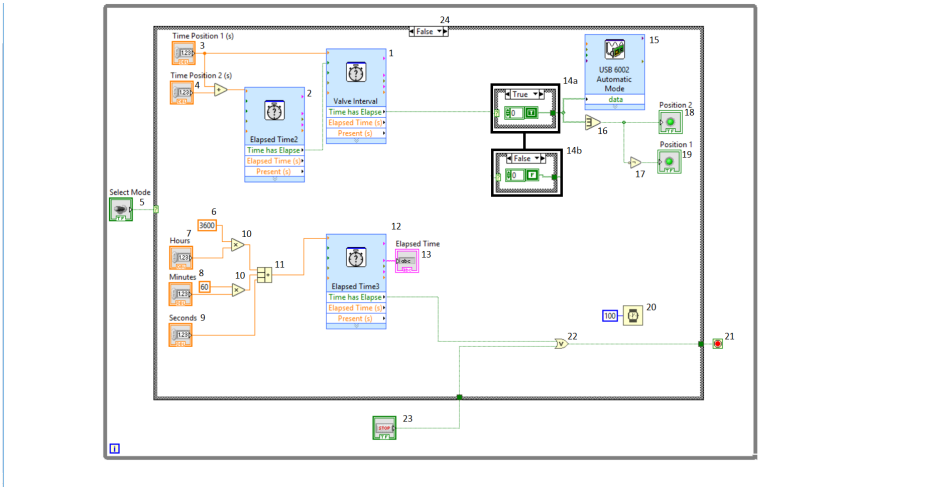


**Figure C.3:** Valve control block diagram with numbered elements.



**Figure C.4:** Valve control front panel with numbered elements.

Figure C.3 shows the block diagram with numbered elements. Element 1 is an *Elapsed Time* sub-VI. This sub-VI outputs a boolean signal according to whether the time set in element 3 is reached. Element 3 gets its number from a control in the front panel, meaning its value is set by the user. As long as its time is not reached, it outputs false. Element 2 is an *Elapsed Time* sub-VI which has a target time equal to the time set in both element 3 plus the time set in element 4. When this time is reached, it resets the timer in element 1. Element 2 is set to auto-reset, meaning that it resets itself when its target time is reached. This way, element 1 starts outputting false to element 14. When the time of element 3 is reached, it outputs true to element 14. When the time of both element 3 and 4 is reached, element two sends a true signal for a split second, before it resets itself. This true signal resets element 1, and element 1 starts outputting false to element 14 again.

Element 14 is a case structure, which is a structure which allows you to have two or more cases, and which case is active is controlled by the input into the little green question mark on the left. The function of this specific case structure is to convert a simple boolean signal (on or off) into a boolean array. A boolean array contains several boolean signals. This case sends a 1x1 matrix containing one boolean signal. This is necessary because element 15 accepts a boolean array and not a simple boolean signal.

---

Element 15 is a sub-VI representing the physical USB interface used to output a signal to the solenoid valve. It is set to output the signal it receives in the *Data*-port. The solenoid valve is two-positional, so when element 15 outputs false, no signal is sent to the valve. This keeps the valve in position 1. When it outputs true, a signal is sent to the valve, and the valve switches to position 2. Element 16 converts a boolean array to a simple boolean signal. This signal is sent to element 18. This is a light diode which can be seen in the front panel which lights up when it receives a true signal. Element 17 inverts the signal which is sent to element 19. These diodes are used as indicators of the valve position.

Elements 7, 8, and 9 are input numbers like elements 3 and 4. These are used to set the time for how long the experiment is run. Element 10 is a simple numerical operator. It gets two number inputs and multiplies them and outputs the product. Element 10 is used together with element 6a and 6b to convert the input from hours and minutes to seconds. Element 11 is a numerical operator which can take several inputs and perform the same operation on all. This specific one adds all inputs. The output is the total number of seconds the experiment shall run for. This is input to element 12, another *Elapsed Time* sub-VI.

Element 12 outputs the time which has elapsed as a text-string. This is shown in the front panel. When time has elapsed, it sends a true signal to element 21. Element 21 is a *Loop Condition* element. When this receives a true signal, the loop it is inside stops. This stops the whole VI. So when the wanted run-time is reached, the experiment stops. Element 22 is a boolean OR-operator. It outputs the same as one or both input signals. So it will output true if either element 12, 23, or both outputs true. Otherwise it will output false.

Element 5 is a boolean switch which is controlled from the front panel. This switch controls the case structure which contains most of the elements, element 24. Figure C.5 shows the other case of the case structure. This is used for manual mode where the user can manually switch the valve position. This is done using the boolean switch shown as element 25 in figures C.4 and C.5.

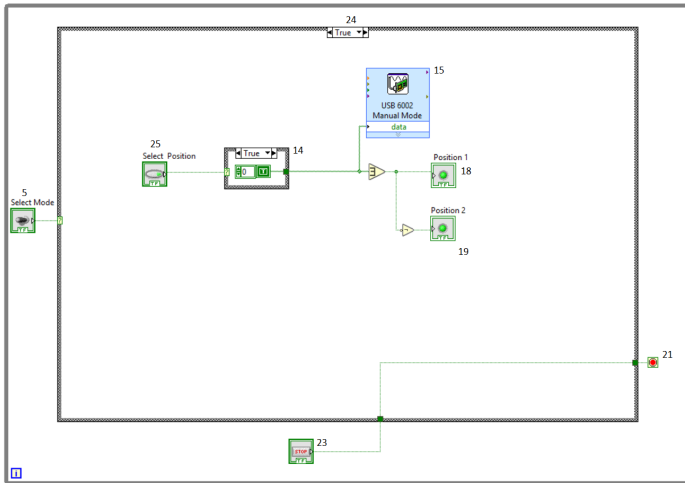


**Figure C.5:** Valve control block diagram with numbered elements.